

Politecnico di Torino



**Politecnico
di Torino**

Laurea Magistrale in Ingegneria Civile

A.A. 2023/2024

Master's Degree Thesis

Modeling and Understanding Flow Transients in Unusual Cases in Water Systems.

Relatori

*Professor Riccardo Vesipa
(Politecnico di Torino)*

*Professor Richard Perkins
(Ecole Centrale de Lyon)*

Candidato

Moustafa Assaf

July 2024



Politecnico
di Torino





Politecnico
di Torino



“...c'est ce contact brutal entre deux mondes : d'un côté celui de la technologie, de l'autre celui de la magie...”

-Rachid Boudjedra



Acknowledgments

I would like to express my deepest gratitude to all those who have supported and guided me throughout the journey of completing this thesis.

First and foremost, I would like to extend my heartfelt thanks to my professor at Politecnico di Torino, Professor Riccardo Vesipa, for providing me with the invaluable opportunity to undertake this research and for his unwavering support and guidance. His encouragement and belief in my potential allowed me to pursue this study at the prestigious École Centrale de Lyon.

I am profoundly grateful to Professor Richard Perkins at École Centrale de Lyon for his mentorship and collaboration on this experiment. His expertise and insights were instrumental in the success of this research. I am truly honored to have had the opportunity to work with such a distinguished scholar.

I would also like to extend my gratitude to my Italian friends and colleagues in Torino, especially Khayal, Martina, Adriana, Daniele, and Marta, for their unwavering friendship and support. Our shared experiences and memories, from exploring Torino together to adventures in Paris and Kraków with Khayal, and Lyon with Adriana and Martina, have made my academic journey not only enjoyable but also memorable.

My deepest appreciation goes to my friends and the wonderful community at my residence for their constant encouragement and support. Your companionship has been a source of strength and motivation.

Lastly, I am forever indebted to my family for their unconditional love and unwavering support. Their faith in me has been the foundation of my achievements, and their sacrifices have made this journey possible. I am especially grateful to my siblings, Mayar and Ali, my father, Ahmad, and my mother, Nisrine.

I extend my sincere thanks to all those who have contributed to my academic and personal growth. Your support has been invaluable in helping me reach this milestone.

Thank you all.

Moustafa



Contents

1. Introduction.....	10
2. Literature Review	11
3. Historical Disasters and Incidents	13
3. Surge Tanks	16
4. Analytical History.....	17
5. Water Hammer Apparatus Overview.....	20
5.1 Brief description.....	20
5.2 Main Phenomena and results :	26
5.3 Applications, Outcomes, and Goals:.....	26
5.4 The current experiment setup and objective in the LMFA	27
6. Experiment's Application and Results.....	28
7. System Installation and Configuration	32
7.1 Numerical Analysis.....	33
8. Method of the characteristics	38
8.1 Brief Description	38
8.2 Mathematical derivation.....	39



8.3 Application and Results.....	46
9. Stability check.....	49
9.1 Ultrasonic Sensors.....	49
9.2 Ultrasonic Sensor Description	50
9.3 Senix Ultrasonic Sensor Selection.....	51
9.3.1 Company Introduction.....	51
9.3.2 Senix Products	52
9.3.3 Optimization and Filtering	55
9.4 Pressure Measurement.....	55
9.4.1 Pressure Measurement Sensor.....	56
9.5 Alternative Methodologies	57
10. Valves	58
10.1 Brief Description of Valves.....	58
10.2 Valves	58
10.3 Valve selection	60
10.3.1 Company Introduction	60
10.3.2 Electro-valve 221G/15.....	60
10.4 Simulation in case of a full-flow.....	62
10.5 Alternative Valves.....	66
11. Conclusion and Future Work	67
12. References	69

Table of Figures

Figure 1 Penstock collapse at Oigawa hydropower plant in 1950.....	13
Figure 2 Cracks in the inlet of the valve of Big Creek	14
Figure 3 The Broken Pump casing in Azambuja Pump Station.....	15
Figure 4 The fallen penstock of Lutschinen Hydroelectric Power Plant	15
Figure 5 Lastioulles equilibrium chimney [2]	16
Figure 6 The two pipes of the experiment	20
Figure 7 Water Reservoir of the experiment	21
Figure 8 The inlet of the water reservoir and the outlet of the spillway	21
Figure 9 Spillway inside the Water Reservoir	21
Figure 10 The Transparent Surge Shaft (equilibrium chimney)	22
Figure 11 Slow closing valve	22
Figure 12 Fast closing valve	23
Figure 13 Keys used to control the water flow velocity	23
Figure 14 A pressure sensor installed in the middle of the second pipe.....	24
Figure 15 A pressure sensor installed at the end of the second pipe	24
Figure 16 The computer and the receiver of the pressure sensor signals	25
Figure 17 Water pump used to pump water in the water reservoir	25
Figure 18 The chimney and observation of results	28
Figure 19 The 8th frame of the water level variation for the first case at 0.24 seconds from the beginning of the experiment	29
Figure 20 Water level variation in the chimney valuation over time for a flow $8 \times 10^{-4} m^3 / s$	30
Figure 21 Water level variation in the chimney valuation over time for a flow $1.7 \times 10^{-4} m^3 / s$	30
Figure 22 Water level variation in the chimney valuation over time for a flow $2.6 \times 10^{-4} m^3 / s$	31
Figure 23 Water level variation in the chimney valuation over time for a flow $4.2 \times 10^{-4} m^3 / s$	31
Figure 24 Water Hammer Experiment Setup in the Laboratory	32
Figure 25 Scheme of the Water Hammer Experiment.....	32
Figure 26 Simulation for a normal case for a flow rate equal to $8 \times 10^{-4} m^3 / s$	35
Figure 27 Simulation in case of the formula is updated for a flow rate equal to $8 \times 10^{-4} m^3 / s$	36
Figure 28 Simulation for a flow rate equal to $1.7 \times 10^{-4} m^3 / s$	37
Figure 29 Simulation for a flow rate equal to $2.6 \times 10^{-4} m^3 / s$	37
Figure 30 Simulation for a flow rate equal to $4.2 \times 10^{-4} m^3 / s$	38
Figure 31 Characteristic lines in x-t plane.....	41
Figure 32 Pipe system	42
Figure 33 Excitation at the downstream end	43
Figure 34 Excitation at the upstream and downstream ends	43
Figure 35 Characteristic Grid.....	45
Figure 36 Simulation of the MOC for a flow equal to $8 \times 10^{-5} m^3 / s$	47
Figure 37 Simulation of the MOC for a flow equal to $1.7 \times 10^{-4} m^3 / s$	47
Figure 38 Simulation of the MOC for a flow equal to $2.6 \times 10^{-4} m^3 / s$	48



Figure 39 Simulation of the MOC for a flow equal to $4.2 \times 10^{-4} \text{ m}^3 / \text{s}$	48
Figure 40 Ultrasonic sensor measurement scheme [4]	50
Figure 41 Senix Corporation Logo	52
Figure 42 Senix products catalog	52
Figure 43 ThoughSonic 3	53
Figure 44 Reservoir Cross-section	53
Figure 45 Reservoir Measurement	54
Figure 46 Water reservoir side while using the ThoughSonic 3	54
Figure 47 pressure measurement sensor A-10.	56
Figure 48 Parker Lucifer Corporation Logo	60
Figure 49 221 G /15 electro-valve	61
Figure 50 221 G 15 Sections	62
Figure 51 Valve opening area variation in function of time of closure.	63
Figure 52 Simulation in case of a total valve opening.....	64
Figure 53 Valves catalog.....	65
Figure 54 All Valve opening and closing times.	65
Figure 55 Motor-driven valve [7].....	66



Abstract

Water hammer, a transient pressure surge resulting from sudden changes in fluid flow, poses significant challenges in the design and operation of modern pipeline systems. This study aims to investigate water hammer phenomena through experimental analysis, focusing on understanding the characteristics and mitigating factors of pressure surges in pipeline network experiments in the Ecole Centrale de Lyon laboratory on a water hammer experiment used to teach engineering students about the water hammer phenomena.

The experimental setup consisted of a laboratory-scale pipeline system with pressure sensors and flow meters to capture real-time data during controlled water hammer events. Various operating conditions, including flow velocity, valve closure rate, and pipe material properties, were systematically varied to examine their effects on pressure transients.

Analysis of the experimental results revealed complex pressure wave behaviors, including wave propagation, reflection, and attenuation, influenced by system geometry and fluid properties. The study identified critical parameters governing water hammer intensity and duration, providing insights into the mechanisms underlying pressure surge generation and propagation.

Furthermore, the experimental data were compared with theoretical models and industry standards to validate the accuracy of existing predictive methods and highlight areas for refinement. Practical implications of the findings for pipeline design, operation, and maintenance were discussed, emphasizing the importance of considering water hammer effects in engineering practice to ensure system reliability and integrity.

Overall, this research advances our understanding of water hammer phenomena and provides valuable guidance for engineers and practitioners in effectively managing transient pressures in pipeline systems.

1. Introduction

Water hammer, a transient pressure phenomenon, occurs when a sudden increase in pressure and flow of the fluid (mainly water but not necessarily) in conduits such as pipes due to a change of velocity in the conduits and it's usually the end section of the conduit mostly due to valve closure or sudden pump shutdown. Suddenly putting an obstacle in the way of the flowing fluid causes the deceleration of the fluid in the conduit by compressing the fluid at the end of the downstream generating pressure due to the conversion of the kinetic energy of the fluid into a potential energy, known as pressure surge or water hammer, in the conduit.

This wave pressure is the excess of pressure that the system handles and causes a fluid propagation back and forth through the conduit with the same velocity as the initial flow until this energy is dissipated. The speed of propagation of these waves is close to the speed of sound in the fluid. Still, the amplitude depends greatly on the speed of the flow modification, the faster the change the more significant the forces generated by the pressure waves.

While water hammer happens in daily life, for example when the shower of water tap is turned off quickly, a loud sound can be heard around the house. Knowing that some of its drawbacks are pipe damage by weakening joints and potential for leaks or even pipe bursts and reduction the system efficiency, vibrations can loosen pipe connections and decrease overall system performance, and, while less common and under extreme circumstances, are cavitation and bubble formation within the pipe.

To protect hydraulic circuits against water hammer pressure variations, an equilibrium chimney is installed, usually, a large capacity reservoir, open to the atmosphere called a chimney. The equilibrium chimney is generally installed in the conduit that feeds a turbine or a valve, just upstream of it. Placing it at this point allows it to effectively absorb pressure variations and minimize the risk of water hammer effects, ensuring smoother operation of the hydraulic system.

Water hammer, although potentially harmful, is a well-understood phenomenon. Engineers can create and manage piping systems that reduce the effects of water hammer by knowing its causes and mechanisms. The goal of this research is to offer insightful analysis and workable solutions to reduce the dangers connected to water hammer in a variety of applications.

2. Literature Review

Introduction

The study of water hammer phenomena, particularly using apparatuses such as the AC7 MkII, is critical for understanding and controlling fluid dynamics in various engineering systems. This section reviews existing literature on water hammer effects, methods for measuring water levels, and the role of different valve types in managing fluid flow.

Water Hammer Phenomenon

Water hammer, characterized by a pressure surge when a fluid in motion is forced to stop or change direction suddenly, has been extensively studied in fluid dynamics. Hanif Chaudhry [1] provided comprehensive insights into hydraulic transients, detailing the principles and equations used to model these phenomena. Wood [1] offered a historical perspective on water hammer research, tracing the evolution of understanding and methods used to mitigate its effects.

Measurement Techniques

Accurate measurement of water levels in chimneys and reservoirs is essential for ensuring the stability and validity of fluid dynamics experiments. Traditional methods, such as manometers and ultrasonic sensors, have been well-documented. This study utilized the Thoughtsonic 3 and Waki A-10 pressure sensors, advanced devices that provide high precision and reliability in dynamic environments.

Hanif Chaudhry [1] discussed various measurement techniques for hydraulic systems, highlighting the importance of accuracy in dynamic conditions. Martínez [2] introduced IoT-based real-time monitoring devices, significantly enhancing the reliability and accessibility of water level data in experimental setups.

Valves in Fluid Dynamics

Valves are crucial for controlling fluid flow and mitigating water hammer effects. Traditional slow-closing valves have been effective in reducing transient pressures associated with sudden fluid stops. Zappe [3] extensively documented the design and performance of various valve types, emphasizing their roles in industrial applications.

The advent of solenoid valves represents a significant advancement in valve technology. Solenoid valves, which can be remotely controlled and precisely adjusted, offer enhanced control over fluid dynamics. P. H. Corporation [4] detailed the engineering fundamentals and applications of solenoid valves, highlighting their advantages over traditional valve types. The Danfoss [6] catalog further elaborates on the capabilities of motorized control valves and their applications in fluid dynamics.

Method of Characteristics (MOC)

The Method of Characteristics (MOC) is a powerful analytical tool for predicting fluid dynamics, especially in systems experiencing water hammer. Hanif Chaudhry [1] provides a detailed methodology for applying MOC to hydraulic transients, offering a framework that has been refined over the years. Ghidaoui [5] discussed integrating computational fluid dynamics (CFD) with MOC to enhance the accuracy and efficiency of fluid behavior simulations. These hybrid models leverage the strengths of both MOC and CFD, offering comprehensive insights into complex fluid dynamics.

Gaps in the Literature

Despite significant advancements in understanding water hammer effects, measurement techniques, and valve technologies, several gaps remain. Limited research exists on integrating smart valves with real-time monitoring systems, and further exploration of combined MOC and CFD applications in large-scale systems is needed. Additionally, experimental validation of advanced models in industrial settings is sparse.

Conclusion

The literature review indicates substantial progress in studying water hammer phenomena and the technologies used to manage them. However, integrating modern measurement techniques with advanced valve designs, such as solenoid valves, presents opportunities for further research. This thesis aims to address these gaps by investigating the behavior of the water hammer apparatus AC7 MkII, implementing precise measurement techniques using the Thoughtsonic 3 and Waki A-10 pressure sensors, and evaluating the impact of replacing traditional valves with solenoid valves, all while utilizing the Method of Characteristics for simulation.

3. Historical Disasters and Incidents

Water hammer occurs in almost all water piping systems it can be domestic such as robinet pipes in residential buildings but also in the Industrial environment, particularly in hydropower plants due to the presence of water, a common ground for water hammer cases, and can have devastating drawbacks.

Neglecting the water hammer phenomenon can have very devastating and destructive consequences. History shows many examples of its destructive power:

- The Oigawa Hydropower Plant Incident (1950, Japan):

One of the most common disasters of the water hammer is the Oigawa hydropower station in Japan, causing a catastrophic penstock collapse in 1950. This incident, triggered by a water hammer during a rapid pressure change, resulted in the death of three workers and huge financial repercussions exceeding half a million dollars. The collapse itself stemmed from a sequence of events. The fall of a hydraulic line feeding the penstock created a vacuum upstream of a burst section, leading to the catastrophic failure of the penstock itself. The Oigawa incident caused immediate fatalities and material damage and halted power generation for a significant period, impacting the surrounding community.

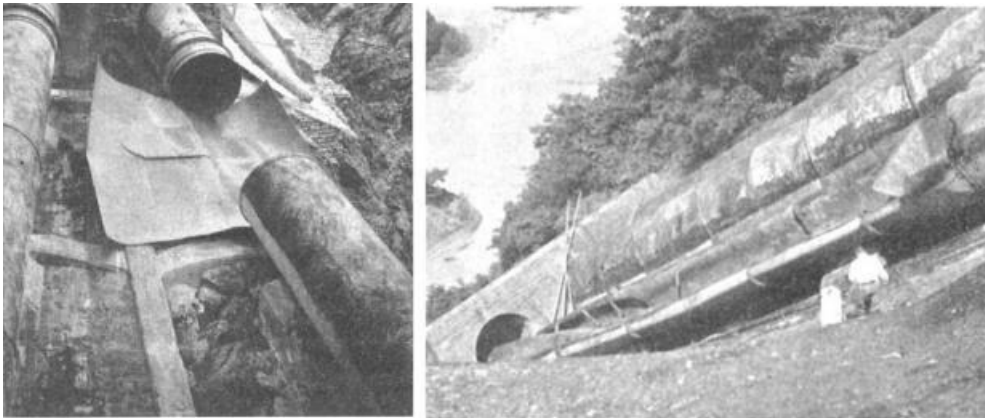


Figure 1 Penstock collapse at Oigawa hydropower plant in 1950

- The Big Creek No. 3 Hydropower Plant Incident (1979,USA):

The United States also has its fair share of water hammer disasters. The Big Creek No. 3 Hydropower Plant experienced a burst turbine inlet valve in 1979 [Trenkle, 1979]. This event occurred very fast. Within three seconds of closing the turbine shut-off valve, the penstock of unit 2 failed catastrophically at a manhole location. The incident occurred while the unit was in service and serving the hydraulic operator of the valve, showing the potential for in case of any human presence around the area. The resulting damage was a crack

in the penstock of a length of 3.7 meters and a width of 76 millimeters. This significant breach in the pressure vessel was due to the force unleashed by water hammer.

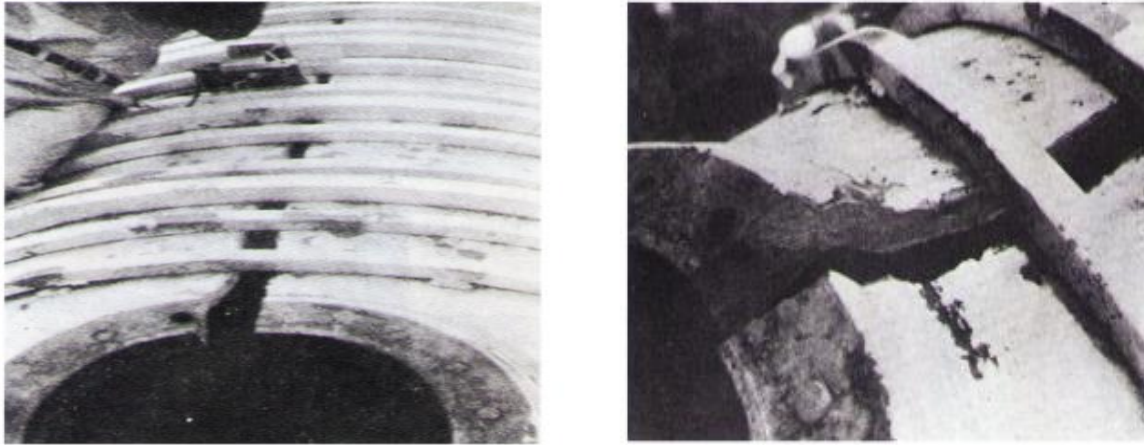


Figure 2 Cracks in the inlet of the valve of Big Creek

These were the two most prominent examples of the water hammer's destructive potential. Other incidents around the world serve as grim reminders:

- Azambuja Pump Station, Portugal: The broken pump casing at the Azambuja Pump Station in Portugal after the occurrence of a burst due to a water column separation.
- Lutschinen Hydroelectric Power Plant, Switzerland: The Lutschinen Hydroelectric Power Plant in Switzerland suffered a fallen penstock due to water hammer effects. , worth mentioning that this occurred during the draining, and the upstream vent was frozen.
- Arequipa Hydroelectric Power Plant, Peru: The Arequipa Hydroelectric Power Plant in Peru also fell victim to the water hammer effect.

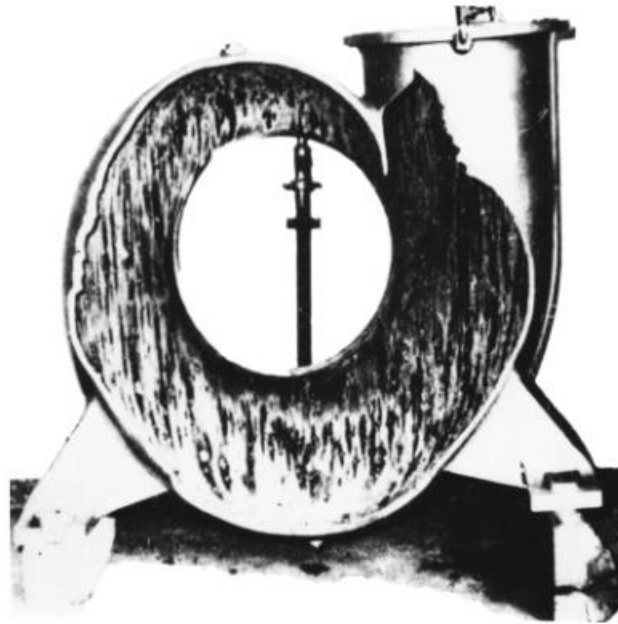


Figure 3 The Broken Pump casing in Azambuja Pump Station



Figure 4 The fallen penstock of Lutschinen Hydroelectric Power Plant

The disastrous results of these past water hammer events prompted the creation of more stringent operational guidelines and design standards. The primary goal of these laws is to increase the global hydropower plant pipe systems' efficiency and, more crucially, safety. The safe and dependable operation of these essential power-producing facilities can be guaranteed by engineers by implementing water hammer mitigation techniques during the hydropower plant design phase, which considerably lowers the chance of catastrophic failures [6].

3. Surge Tanks

Surge tanks emerge as an essential tool to prevent the adverse effects of water hammer and its backlashes. Acting as reservoirs with great capacity, serve as a buffer against these slow pressure surges, ensuring a smoother and more stable operation of the whole hydraulic system (especially in hydropower plants). The surge tank's design and placement are crucial for its effectiveness. Typically, they are built upstream of the turbines or valves, often integrated into the penstock itself (to prevent incidents similar to the ones already mentioned since many of them occurred near or at the penstock). The surge tank absorbs and releases water depending on the surge strength, effectively dampening pressure oscillations, protecting the hydraulic structure and systems from destructive fates, and saving money and human lives.

The implementation of surge tanks has proven to be an invaluable element in preventing the destructive effects of pressure surges. They have become a crucial part of hydropower plants and major hydraulic structure designs, ensuring the smooth and efficient operation of these industrial and power generation facilities [6].



Figure 5 Lastioules equilibrium chimney [7]

One famous surge tank (also known as “Chambre d’équilibre” or “cheminée d’équilibre” in French) is the Lastioules equilibrium chimney in Auvergne-Rhône-Alpes, France with a height and diameter of 75.80 (where 32 meters above the ground) and 6.7 meters respectively. The Lastioules surge tank proves how effective these hydraulic structures can be. Its environmentally friendly design integrated into the surrounding environment, shows the significance of surge tanks in maintaining the stability and reliability of hydropower generation in France [7].

4. Analytical History

Knowing that the historic roots of the water hammer date back to the old times and old civilizations like the Romans ever since they tried to study it harness it and implement it when they were using it to pump water in the public water supply system and distribute it even without having a name of this phenomena.

It was not until 1775 that Euler started studying the water hammer phenomena and it was the blood flow in the arteries in the human body. However, he failed to attain any solution due to the missing analytical and geometrical formulation at that time and nothing could have been accomplished without the development of calculus and the solution of partial differential equations due to change. Since then developments have been done in these domains from the works of René Descartes’s putting geometry on an algebraic basis to Wilhelm Leibniz’s method for partial differential equation solutions.

Diederik Korteweg (1878)

Korteweg was the first scientist to work on wave velocity while taking into account both the pipe wall the fluid inside and the radial acceleration of the pipe walls. That being said, Korteweg was interested only in propagation velocity and not in the transient pressure velocity relationship. So he neglected many key elements related to pressure in the conduit mainly:

- the friction by dealing with pipes in which vibrations are present only from sound and wave.
- longitudinal stresses caused by the bending of the pipe since the wave length is much greater than the pipe diameter.
- The change of pressure with each variation in the modulus of elasticity.

Therefore, the acceleration equation is the following:

$$a = \sqrt{\frac{K/\rho}{1 + (K/E)(D/e)'}}$$

Where each parameter is the following:

K:the bulk modulus

ρ :the mass density

R:the mass density

E:the Young's modulus of the pipe wall material

D:the inner diameter of the pipe

e:the pipe wall thickness

Jules Michaud (1878)

Jules Michaud was considered by some as the first ever scientist to study water hammer but in reality it was not him but Menabrea since Michaud worked heavily on use and design of air chamber and safety valves to prevent surges and protected the pipeline system but did not introduce anything for wave velocity or pressure in the conduits. Yet the formula attributed to him can be applied when the closure time is greater than time the first negative pressure arrives ($T_c > T$ linear total closure) was the following:

$$\Delta H \leq \frac{2L\Delta V}{gT_c}$$

Nikolai Joukowski (1897)

In the summer of 1897 and in the following winter in Moscow and after conducting many experiments on the pressure and velocity during water hammer using 3 loops iron casted pipes and the flow is stopped instantaneously add to that he was a consulting engineer for Moscow water projects. Joukowski derived the famous law for sudden water hammer for a fast cut-off period ($T_c < T$) where pressure is equal:

$$\Delta H = \frac{a\Delta V}{g}$$

It's worth mentioning that the time of reference to T_c is equal to the following:

$$T_c = \frac{4L}{a}$$

Where the parameters are the following:

T= Time of the maneuver in seconds.

T_c = Reference time.

ΔV = Variation of speed in m/s during the time T.

a = Wave speed in m/s.

g = 9.81 m/s².

L = length of the pipe in m.

Gaspard Monge (Graphical Methode) (1789)

Monge, also known as the founder of École Polytechnique, introduced in his journal "Memoire sur l'integration graphique des equations aux derivees partielles" the graphical integration of partial differential equations and called it the characteristic method. That being said Louis Bergeron in 1931 expanded the graphical method to make an analytical relationship between the pressure and the velocity between two points anywhere in the pipeline system. Basically, two positions on the pipes P and Q are chosen with their respective position and time following this formula:

$$(x - at)_P = (x - at)_Q \Rightarrow x_P - x_Q = (t_P - t_Q)$$

And the equation that connects the pressure and the velocities is the following:

$$(H_P - H_Q) = -\frac{a}{g}(V_P - V_Q)$$

Now if the pressure and velocity values (H and V) are known for two positions in the pipe at a given time it's possible to know the pressure and the velocity at these sections later by a time interval Δt .

This a very useful method to deal with pipe networks but in case of junctions and change in section mainly guarantee the continuation of the flow and that the pressure at the junctions are equal.

Even so that in 1932 Schnyder applied the graphical method for pipelines connected to centrifugal pumps in his studies by using complete pump characteristics and was the first to include the friction in the pipe. By drawing a friction curve below the velocity line with an ordinate $-fV^2$ (V is the velocity and $F = \frac{f}{2gD}|V|$ where f is the friction coefficient following D'Arcy parabolic law).

Lorenzo Allievi (1902-1913)

Allievi developed the first formulations set by previous researchers specially Korteweg and got more important formulations by neglecting the term $V \frac{dV}{dx}$ in the continuity equation since he considered it as useless and obtained a second-order equation where its solutions. Add the following formula for maximum pressure rise using the following equation:

$$\frac{h}{H_0} = \frac{1}{2} \left(\frac{\rho}{\theta} \right)^2 \left(1 + \sqrt{4 \left(\frac{\theta}{\rho} \right)^2 + 1} \right)$$

Knowing that " θ " (gate operation or valve closure characteristic) is equal to $\frac{aT_c}{2L}$ and T_c is the equivalent time of date closure.

" ρ " is equal to $\frac{aV_0}{2gH_0}$ and also it's the average of the kinetic and potential energies of water present in pipes at the pressure head H_0 [1].

5. Water Hammer Apparatus Overview

5.1 Brief description

The 'Water Hammer' experiment present in the LMFA laboratory, or 'Experiment du Coup de Bélier' in French, is the Armfield C7 MkII is a self-contained apparatus designed to shed light on the fascinating world of fluid dynamics, specifically focusing on two pressure-related phenomena: pipe surge and water hammer. This experiment is a valuable tool for Professors who want to teach and deliver these concepts and their practical implications in hydraulic systems to their students. Since it's used to investigate the effect of the 'slow' closing or opening of a valve, the amplitude and period of the water level oscillation in the equilibrium chimney of the first conduit are measured.

The Water Hammer experimental setup is composed of the following components:

- **Twin Test Pipes:** The C7 MkII has two test pipes made from stainless steel (to prevent rust and thus minimize friction loss). These pipes serve as the channels through which water flows during experiments and connect the water reservoir to the valves.



Figure 6 The two pipes of the experiment

- Water Reservoir: This tank is the water source for conducting the experiments. It maintains a consistent water level, ensuring a steady flow through the pipes. This consistency is crucial for accurate and repeatable measurements (the dimensions of the water reservoir will be defined later in this document). In the middle of the tank there is a spillway inside to prevent water from flooding and spilling outside the reservoir.



Figure 7 Water Reservoir of the experiment



Figure 9 Spillway inside the Water Reservoir



Figure 8 The inlet of the water reservoir and the outlet of the spillway

- **Transparent Surge Shaft:** One of the pipes includes a transparent surge shaft (also known as the equilibrium chimney or just chimney for short). This shaft is made of acrylic (transparent plastic), allowing for visual observation of the water level variation within the pipe. The surge shaft also features a scale, enabling users to measure the magnitude of these variations.



Figure 10 The Transparent Surge Shaft (equilibrium chimney)

- **Two Valves Control and Flow Speed Keys:** The two valves for water flow control are set at the end of each pipe. A lever-operated valve is positioned at the discharge end of the first pipe. This valve allows for gradual closure, similar to real-world scenarios where valves might be closed slowly. The second valve, which closes rapidly, is installed on the other pipe to demonstrate the impact of rapid closure initiated by a pressure button. Add to that, control over the flow rate within the system before valve closure is provided downstream in both pipes through additional keys.



Figure 11 Slow closing valve



Figure 13 Keys used to control the water flow velocity



Figure 12 Fast closing valve

- Two Pressure Sensors: The apparatus is equipped with two electronic pressure sensors carefully placed on the pipe. One sensor is adjacent to the fast-acting valve and another is placed in the middle of the pipe. These sensors are crucial for capturing the high-speed pressure spikes caused by water hammer as it's almost impossible to realize the phenomenon without the presence of the two sensors.



Figure 15 A pressure sensor installed at the end of the second pipe



Figure 14 A pressure sensor installed in the middle of the second pipe

- **Conditioning Unit and Data Acquisition:** The two pressure sensors are connected to a conditioning unit. This unit processes the sensor signals, making them compatible with PC software for further to be able to see the results and analyze them. The conditioning unit is connected via a USB connection, allowing for data transfer to the computer.



Figure 16 The computer and the receiver of the pressure sensor signals



Figure 17 Water pump used to pump water in the water reservoir

5.2 Main Phenomena and results :

- **Pipe Surge:** The first pipe with its transparent surge shaft takes center stage for investigating pipe surge. By manipulating the flow rate using the keys and then closing the lever-operated valve, users can induce slow changes in water velocity. These oscillations corresponds to the changes in pressure, which are described as variations in the water level within the surge shaft.
- **Water Hammer:** The water hammer phenomenon occurs in the second pipe. This phenomenon occurs due to rapid changes in fluid velocity. This is done using the experiment's fast closure valve. When this valve is closed, a pressure surge, known as water hammer, travels back and forth through the pipe due to the sudden closure of the valve and thus changes in velocity and thus the change in water pressure. The two pressure sensors positioned along the pipe capture the characteristics of this pressure wave. By deducing the time delay between the readings from the two sensors, the speed of sound in the water can be determined.

5.3 Applications, Outcomes, and Goals:

This experiment serves as a pivotal tool for comprehending the dynamics of pipe surge and water hammer for students. These phenomena can have direct consequences in real-world applications involving pipelines and water distribution systems. Pipe surge can lead to unwanted pressure changes and potential damage to pipework components or even destruction of pumps. Water hammer, with its even more rapid pressure spikes, poses a serious threat to pipe integrity if not properly accounted for in the design. By studying these phenomena using the C7 MkII, engineering students can gain valuable insights and knowledge that can be applied to:

- **Optimization of pipeline network systems:** Understanding the pressure variations caused by surge and hammer allows engineers to design pipelines that can withstand these forces, improving their overall reliability and lifespan of the systems.

- Proper valve selection: The C7 MkII demonstrates the impact of valve closure speed on pressure transients. This knowledge helps engineers choose valves that minimize surge and hammer effects in real-world systems all while being economical in the selection in terms of cost and feasibility.
- Implementing surge protection methods: The apparatus can be used to evaluate the effectiveness of various surge protection measures, such as surge tanks or air chambers, in mitigating pressure fluctuations.

All in all, the Armfield C7 MkII Pipe Surge and Water Hammer Apparatus offer a comprehensive and practical learning environment for exploring the intricacies of fluid flow behavior in pipes. By enabling the visualization and measurement of pressure variations associated with surge and hammer, this equipment empowers engineers and researchers to design safer and more efficient hydraulic systems.

5.4 The current experiment setup and objective in the LMFA

The experiment apparatus in the laboratory of the Laboratoire de Mécanique des Fluides et d'Acoustique (LMFA) at the Ecole Centrale de Lyon consists primarily of all the already mentioned components and is preserved in a good condition that is still being used today to teach the students fluid dynamics.

Yet the administration of the LMFA - Fluid Mechanics and Acoustics Laboratory decided to check the stability of the apparatus if it was properly calibrated and stable. Plus improving the experiment and applying some changes like replacing the slow closing valve with a new valve that uses modern technology to open and close to better show and teach the students the water hammer phenomena and better under since it had not been changed for more than 30 years.

Even the gradual closing of a valve within a pipe initiates a pressure wave, commonly referred to as a 'surge wave' or 'pipe surge,' necessitating effective damping. This experimental setup offers a visual representation of how an equilibrium chimney operates to mitigate the impact of the pressure wave.

Measuring both the amplitude and period of the pressure wave allows for a comparison with theoretical expectations. This process aids in comprehending and confirming the equilibrium chimney's efficiency in attenuating the effects of the pressure wave [8].

6. Experiment's Application and Results

The experiment was conducted for 4 different flow rates of 8×10^{-5} , 1.7×10^{-4} , 2.6×10^{-4} , and 4.2×10^{-4} all in m^3 / s . During each scenario, the water flow was set to a specific speed. When the slow-closing valve is closed, the water stops flowing in the pipe and the water level rises in the equilibrium chimney. This process is video registered for each scenario and the video is divided into frames depending on the registration device, in this case, a budget telephone camera was used with an average resolution.

Then based on the camera's frame rate, the video was divided into photos where each illustrating the water level at a specific time of the experiment. Thus, the output is a compilation of the dataset, representing the oscillation amplitudes at each specified flow rate at a certain time of the experiment. This approach provides a clear representation of the oscillation behavior of the water level with each different flow rate.

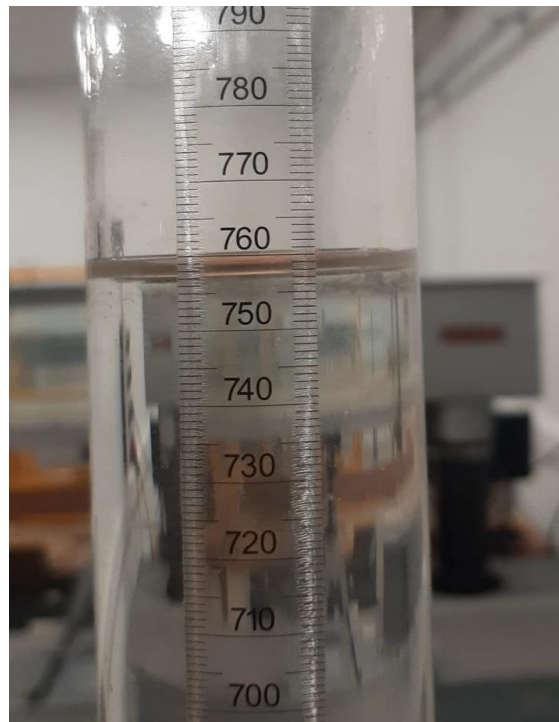


Figure 18 The chimney and observation of results

For the best accuracy possible the video of each experiment was divided into images using Matlab based on the frame of each video so that it was easy to track the water level variation and have a better resolution. The collected data are usually the local maximum and minimum oscillations and a few midpoints of each local oscillation for the best representation as this will help in the interpolation.

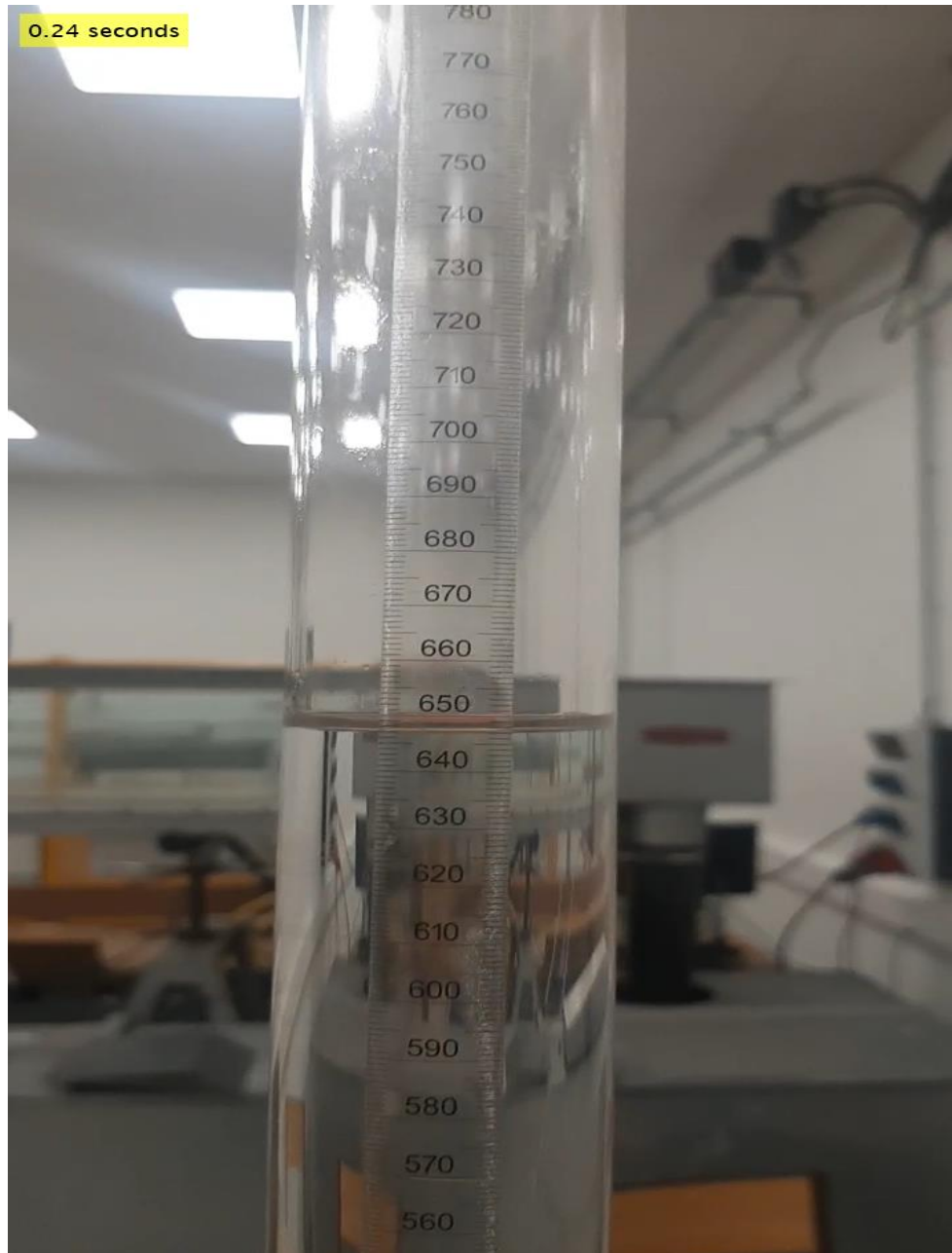


Figure 19 The 8th frame of the water level variation for the first case at 0.24 seconds from the beginning of the experiment

The following graphs represent the water level variation for each case throughout the experiment. This is done by inserting the observed water variation into Matlab and requesting an interpolation so that it is possible to

observe the level variation from the beginning to the end of the experiment without any missing data (gaps) so that it's possible to compare it later with the analytical data.

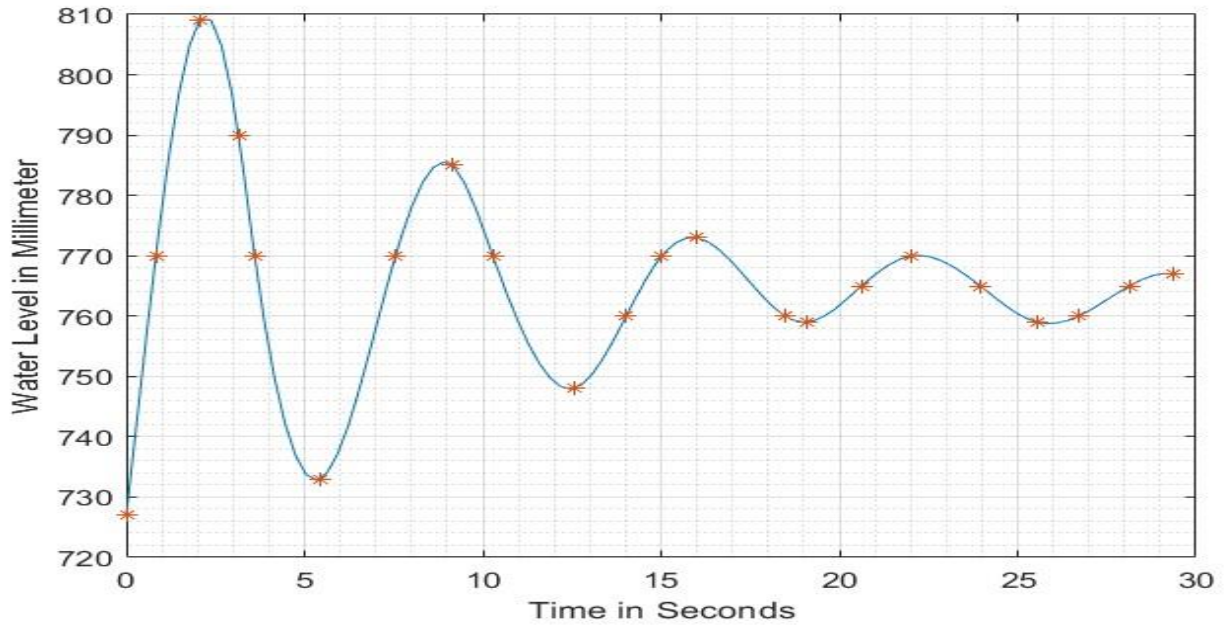


Figure 20 Water level variation in the chimney valuation over time for a flow $8 \times 10^{-4} \text{ m}^3 / \text{s}$

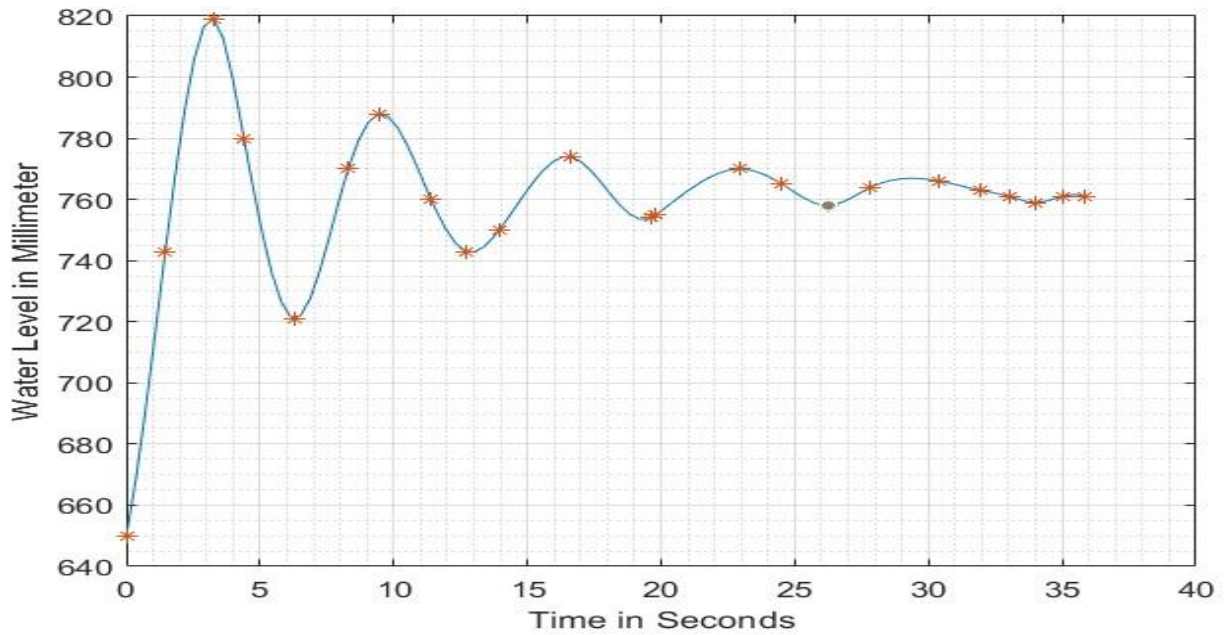


Figure 21 Water level variation in the chimney valuation over time for a flow $1.7 \times 10^4 \text{ m}^3 / \text{s}$

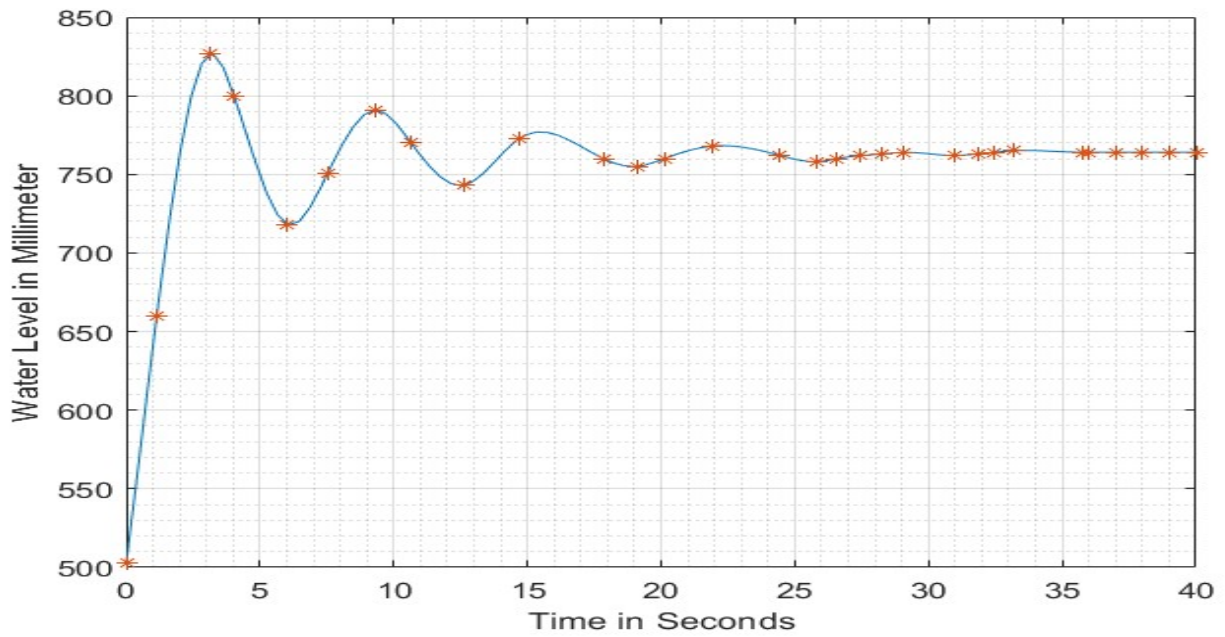


Figure 22 Water level variation in the chimney valuation over time for a flow $2.6 \times 10^{-4} \text{ m}^3 / \text{s}$

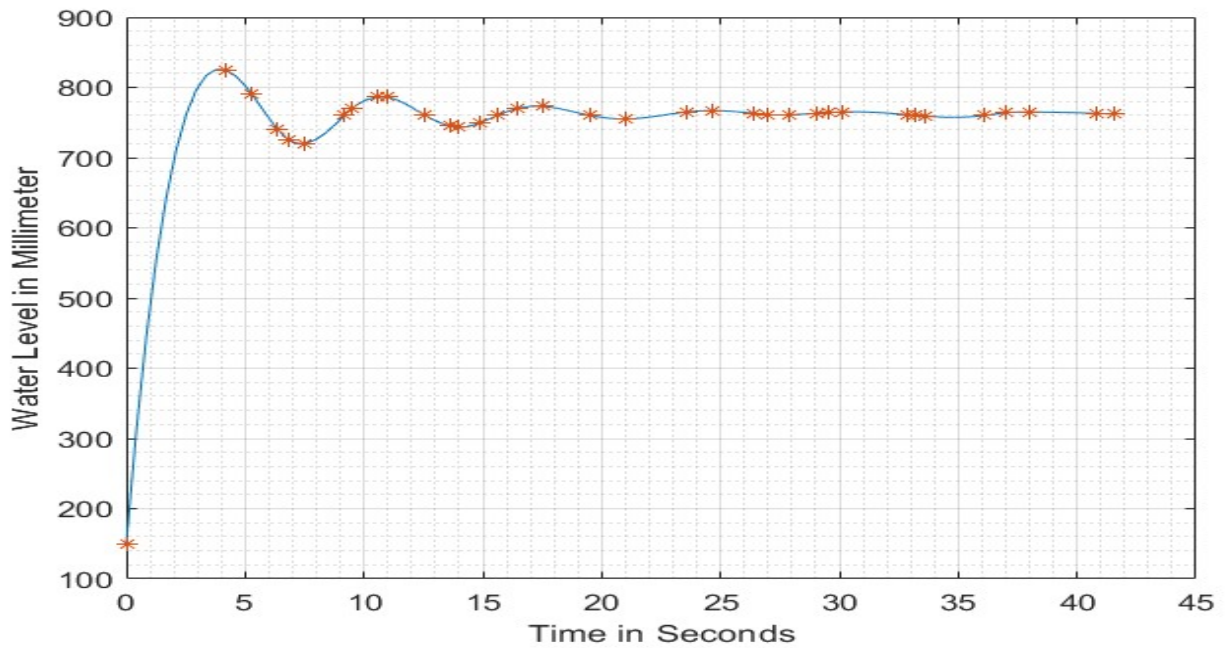


Figure 23 Water level variation in the chimney valuation over time for a flow $4.2 \times 10^{-4} \text{ m}^3 / \text{s}$

These outputs forms the benchmark foundation for the analysis, and be used as a milestone to make comparisons between the observed and analytical results. This comparison between the observed data and analytical simulations represents the accuracy and the robustness of the experiment.

7. System Installation and Configuration

To better understand the experiment installation, a scheme of the apparatus setup was drawn (using AutoCAD) to illustrate in a drawn AutoCAD scheme below. This drawing illustrates all components' precise dimensions and specifications to ensure accuracy in both numerical analysis and future development.



Figure 24 Water Hammer Experiment Setup in the Laboratory

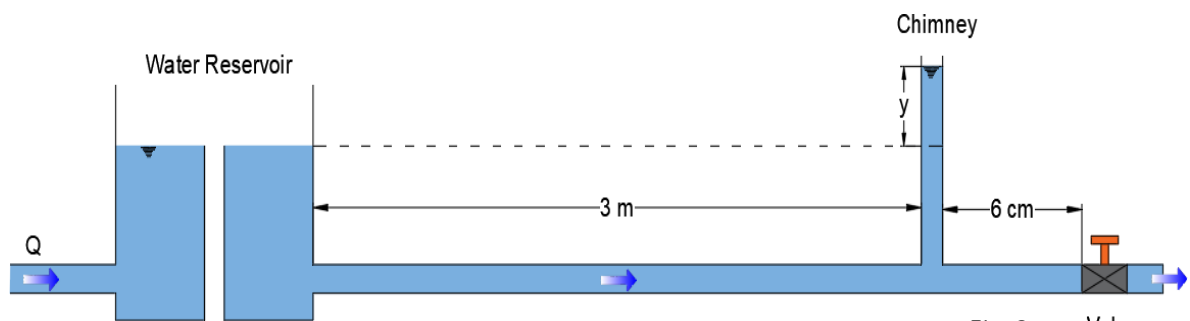


Figure 25 Scheme of the Water Hammer Experiment

The details and dimensions of the experiment of the following components:

1. Manual valve with slow closing and opening.
2. Equilibrium chimney
 - Internal diameter = 44.0 mm
3. Pipe 1 (between the water reservoir and the chimney):
 - Diameter = 20.2 mm
 - Wall thickness = 0.90 mm
 - Length = 3.0 m
 - Equivalent Roughness = 0.0075 mm
4. Pipe 2 (between the chimney and the slow-closing valve):
 - Diameter = 20.2 mm
 - Wall thickness = 0.90 mm
 - Length = 6 cm
 - Equivalent Roughness = 0.0075 mm
5. Water Reservoir:
 - Inner Diameter = 26 cm
 - Length = 93.0 m

7.1 Numerical Analysis

In the water hammer experiment, numerical analysis is required to provide insights into the system's dynamic behavior. When focusing on the slow closure of the valve, numerical simulations play an essential role in understanding the amplitude and period of pressure waves. Using finite difference or finite volume methods, it's possible to computationally model the experiment's mathematical framework. These numerical approximations allow the prediction and analysis of water level variations, paving the way for a deeper exploration of transient pressure surges. This introduction prepares us for the subsequent inclusion of specific formulas, offering a quantitative perspective on the investigation.

Applying the balance of forces on the system is like a rigid conduit enabling the derivation of a formulation that influences the oscillation within the system. This fundamental approach allows the systematic analysis and quantifies the dynamic interactions of forces acting on the experimental setup.

Using Newton's second law over the standard conduit :

$$\rho AL \frac{dv}{dt} = \rho g A h_1 + \rho g A L \sin(\theta) - \rho g A (h_2 + y) - \rho g A h_f$$

Where the parameter is the following:

A: Cross-section area

v: Mean velocity

L: Length of the conduit

ρ : Fluid density

y: Variation of level in the water chimney

θ : The inclination angle of the pipe connecting the reservoir to the valve (in the current experiment is equal to 0)

h_1 : Water level in the reservoir

h_t : Pressure loss in the conduit in the conduit

g: Gravity coefficient

$$\frac{L}{g} \frac{dv}{dt} = -(h_f + y)$$

Where h_f is the friction loss and it is equal to:

$$h_f = -\frac{\lambda L}{g_a} v^2$$

By substituting with the conservation of mass formula we get the following equations:

$$\frac{d^2 y}{dt^2} = \frac{gA}{LS} \left[\frac{\lambda L}{g_a} \left(\frac{dy}{dt} \right)^2 - y \right]$$

This nonlinear equation can't be solved analytically; therefore, we resort to other numerical methods for its solution. But by neglecting the friction factor it is possible to get the following results:

$$\frac{d^2 y}{dt^2} + \frac{gA}{LS} y = 0$$

This equation is nonlinear in y and a nonlinear function of velocity, $\frac{dy}{dt}$, meaning there is no analytical solution. However, if we neglect the friction losses, we obtain the classical equation for harmonic oscillation:

The solutions are the following:

$$y = Y \sin(\omega t)$$

$$Y = v \sqrt{\frac{LA}{gS}}$$

$$\omega = v \sqrt{\frac{gA}{LS}}$$

Using MATLAB software it's possible to solve this nonlinear equation and obtain results. However, while these results are mathematically correct, they are physically inaccurate. When water flows in the opposite direction, friction should oppose the motion. Instead, the current results incorrectly show friction aiding the motion, leading to an increase in flow speed in the chimney over time rather than the expected decrease.

Applying this formula for the case of 8×10^{-5} gives the following results:

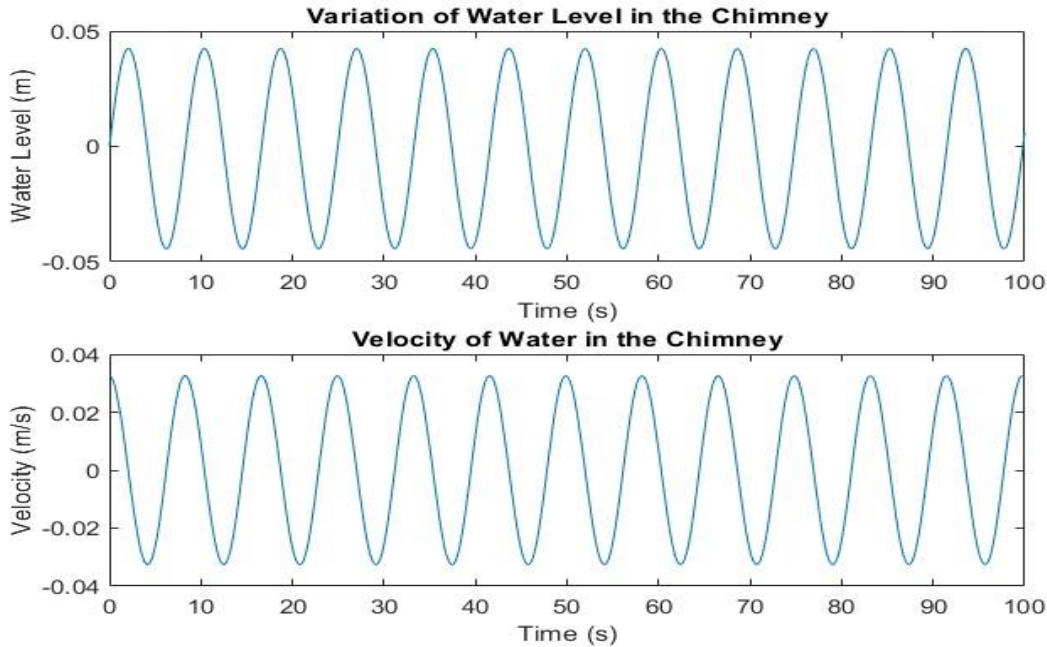


Figure 26 Simulation for a normal case for a flow rate equal to $8 \times 10^{-4} \text{ m}^3 / \text{s}$

Meanwhile, if the formula is adjusted to this to its proper physical meaning it will be equal to the following:

$$\frac{d^2y}{dt^2} = \frac{gA}{LS} \left[\frac{\lambda L}{ga} \left(\frac{dy}{dt} \right) \left(\left| \frac{dy}{dt} \right| \right) - y \right]$$

In this formulation, the velocity adopts the sign and direction of the flow, ensuring physical accuracy and resulting in proper values and simulations. This approach corrects the physical representation of the system dynamics and leads to more realistic simulation outcomes. By considering the actual flow direction and velocity, the model provides a more accurate depiction of the system's behavior.

This is the simulation for the case of a flow rate equal to $8 \times 10^{-4} \text{ m}^3 / \text{s}$:

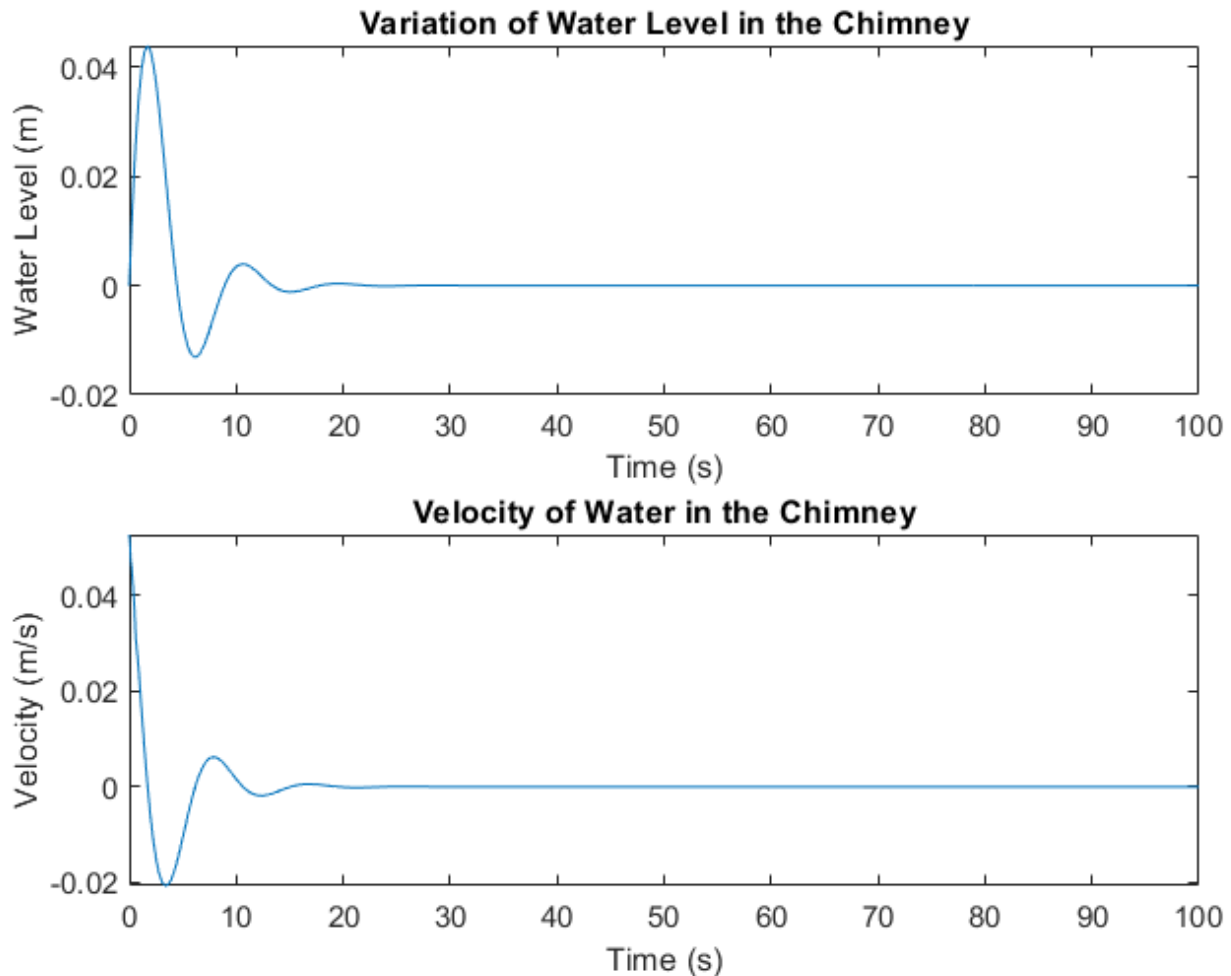


Figure 27 Simulation in case of the formula is updated for a flow rate equal to $8 \times 10^{-4} \text{ m}^3 / \text{s}$

It can be noticed that the water level and the velocity in the chimney decrease gradually over time which goes perfectly with what we have seen while conducting the experiment and the obtained result aligns with the experimental output, especially the oscillation period T that varies between .

The same simulation has been conducted for all three other scenarios with different flow rates and the results are the following:

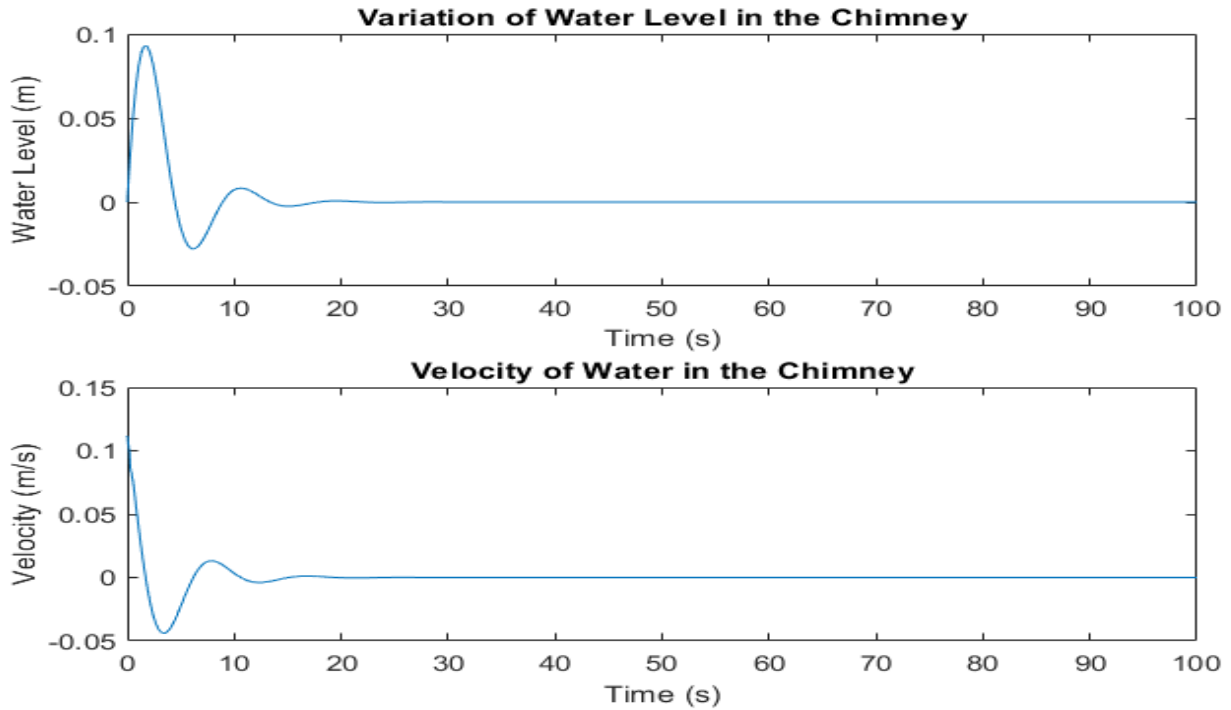


Figure 28 Simulation for a flow rate equal to $1.7 \times 10^{-4} m^3 / s$

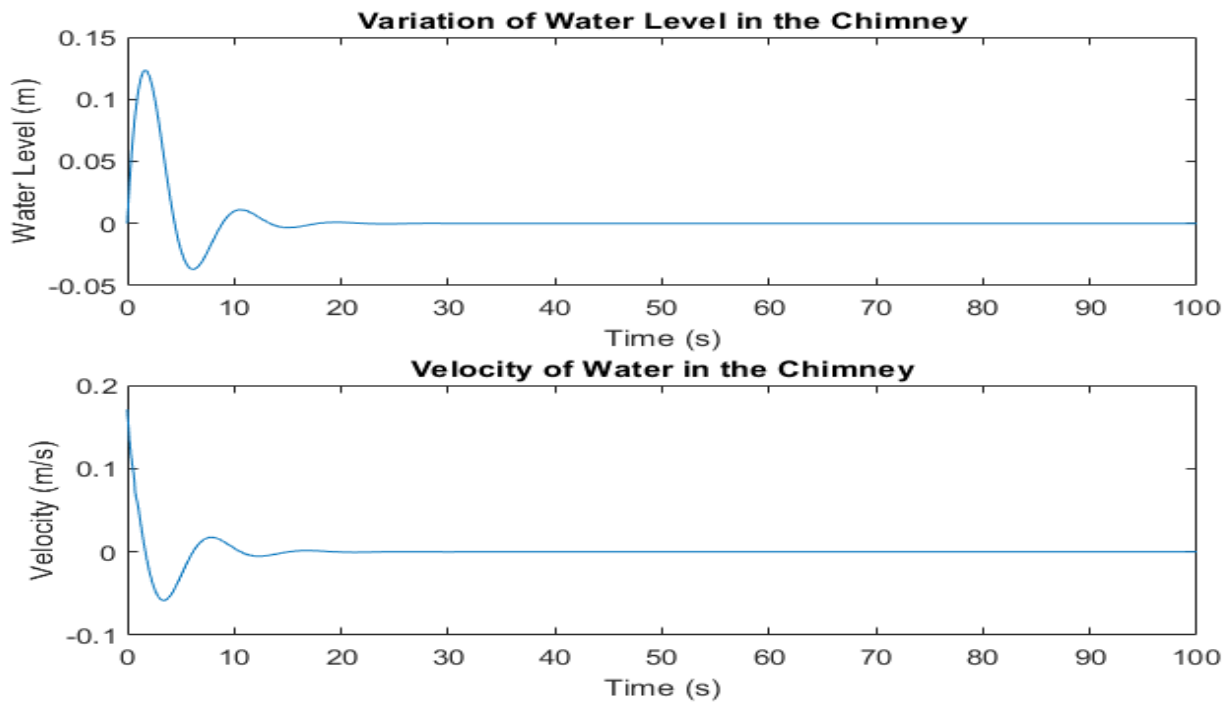


Figure 29 Simulation for a flow rate equal to $2.6 \times 10^{-4} m^3 / s$

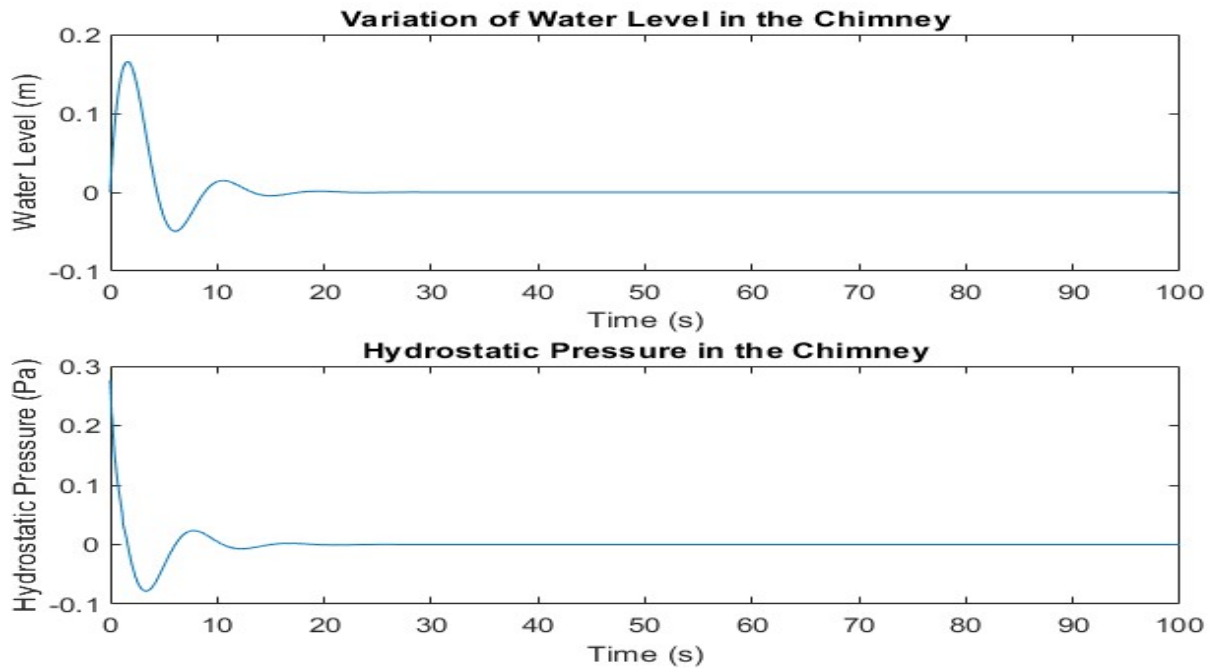


Figure 30 Simulation for a flow rate equal to $4.2 \times 10^{-4} m^3 / s$

It can be witnessed that the higher the flow rate in the pipes the greater the oscillation in the chimney in terms of water level and velocity and this is because a high flow rate causes a bigger pressure surge thus the chimney plays the role of a surge tank and the water level goes higher to dissipate the generated pressure caused by the water hammer phenomena.

8. Method of the characteristics

8.1 Brief Description

The method of characteristics, or MOC for short, is a mathematical method used to solve partial differential equations, especially those describing wave-like phenomena. It consists of converting the partial differential equation into a set of ordinary differential equations along characteristic curves, allowing for the prediction of how waves or other phenomena propagate through a system. This approach is considered a strong tool for assessing and forecasting fluid dynamics behavior.

Additionally, using the method of characteristics gives us the ability to successfully modify the system and understand its dynamics. This includes the possibility of substituting any element of the system and even

adding new ones to the system, for example, changing the valve with new ones or changing their initial opening and checking how this will affect the output and the whole system.

8.2 Mathematical derivation

The method of characteristics is an approach widely used in hydraulic engineering to study one-dimensional flow patterns in open channels and pipes. Known for its effectiveness in solving differential equations this method provides a structured framework for comprehending the intricate flow dynamics within hydraulic systems.

Essentially the method of characteristics involves defining curves that illustrate how waves propagate throughout the flow area. By integrating the governing equations along these curves the original partial differential equations are converted into a set of equations simplifying the solution process.

A crucial aspect of this technique is applying conditions along these curves, which determine how the solution behaves at the boundaries of the flow area. These conditions typically involve specifying parameters like flow rate and water level.

After integrating and applying conditions the solution is reconstructed by combining information gathered from characteristic paths. The method of characteristics excels in handling flow scenarios and discontinuities proving essential for simulating hydraulic events such, as flood waves and hydraulic transients.

In conclusion, the method of characteristics proves to be a flexible tool, in hydraulic engineering providing a way to examine and address intricate flow issues controlled by hyperbolic partial differential equations.

The derivation to reach the applied methods of the characteristics is as follows:

Knowing that the momentum equation is the following:

$$L_1 = \frac{dQ}{dt} + \frac{dH}{dx} gA + \frac{f}{2DA} Q|Q| = 0$$

Considering the $R = \frac{f}{2DA}$

The continuity equation is :

$$L_2 = a^2 \frac{dQ}{dx} + \frac{dH}{dt} gA = 0$$

Applying a linear combination of both equations L_1 and L_2 (continuity and momentum equations) will result in an equation called “L”.

Thus:

$$L = L_1 + \lambda L_2 = 0$$

λ is an unknown multiplier to be defined, so the resulting equation is valid.

$$\left(\frac{dQ}{dt} + \lambda a^2 \frac{dQ}{dx}\right) + gA\lambda \left(\frac{dH}{dx} + \frac{dH}{\lambda dt}\right) + RQ|Q| = 0$$

$$L = \frac{dQ}{dt} + gA\lambda \frac{dH}{dt} + RQ|Q| = 0$$

Since $H = H(x,t)$ and $Q = Q(x,t)$ this implies that the total derivation of the equations is as follows:

$$\frac{dQ}{dt} = \frac{dQ}{dt} + \frac{dQ}{dx} \frac{dx}{dt}$$

$$\frac{dQ}{dt} + \lambda a^2 \frac{dQ}{dx} = \frac{dQ}{dt} + \frac{dQ}{dx} \frac{dx}{dt} = \frac{dQ}{dt}$$

Defining the unknown multiplier λ as such:

$$\frac{1}{\lambda} = \frac{dx}{dt} = \lambda a^2$$

Meaning that :

$$\lambda = \pm \frac{1}{a}$$

Replacing $\frac{dQ}{dx}$ and $\frac{dQ}{dt}$ with $\frac{dQ}{dt}$ but this limitation is introduced in that $\frac{dx}{dt} = \lambda a^2$.

$$\frac{dH}{dt} + \frac{dH}{\lambda dx} = \frac{dH}{dt} + \frac{dH}{dx} \frac{dx}{dt} = \frac{dH}{dt}$$

In case $\frac{1}{\lambda} = \frac{dx}{dt}$

Thus:

$$L = \frac{dQ}{dt} + gA\lambda \frac{dH}{dt} + RQ|Q| = 0$$

Yet if $\lambda a^2 = \frac{dx}{dt}$ and $\frac{1}{\lambda} = \frac{dx}{dt}$

Implies that:

$$\frac{1}{\lambda} = \frac{dx}{dt} = \lambda a^2 \quad \text{Means that} \quad \frac{dx}{dt} = \pm a \quad \text{and} \quad \lambda = \pm a$$

Thus: $\frac{dQ}{dt} + gA \frac{dH}{a dt} + RQ|Q|=0$ if $\frac{1}{\lambda} = \frac{dx}{dt} = a$

And $\frac{dQ}{dt} + gA \frac{dH}{-a dt} + RQ|Q|=0$ if $\frac{dx}{dt} = -a$

Known that the system of partial differential equations (PDEs) is a simpler system of ordinary differential equations (ODE). But the PDE is valid for any value of $\frac{dx}{dt}$ while the ODE is valid only for $\frac{dx}{dt} = -a$ meaning that for a straight line (if a is constant).

These 2 equations are known as the compatibility equations. In the x - t plane, Equations $\frac{dx}{dt} = -a$ and $\frac{dx}{dt} = a$ define two straight lines with slopes of $\pm a$, known as characteristic lines. These lines mathematically partition the x - t plane into two regions, potentially dominated by different solutions, resulting in discontinuities along these lines. Physically, these lines indicate the paths followed by disturbances in the x - t plane. For instance, a disturbance originating at point A (Figure 32) at time t_0 travels along line AP and arrives at point P after a time interval Δt . The next step involves solving the compatibility equations along the characteristic lines, solving the equations $\frac{dQ}{dt} + gA \frac{dH}{a dt} + RQ|Q|=0$ (known as equation 4.1) and $\frac{dQ}{dt} + gA \frac{dH}{-a dt} + RQ|Q|=0$ (known as equation 4.2), it is essential to discuss the physical significance of characteristic lines in the x - t plane. These equations, when integrated, provide a means to determine variables such as flow rate (Q) and head (H) at any point in the flow domain.

The process begins by formulating the compatibility equations based on the governing equations of motion and continuity specific to the hydraulic system. These equations must be valid along the characteristic lines in the x - t plane.

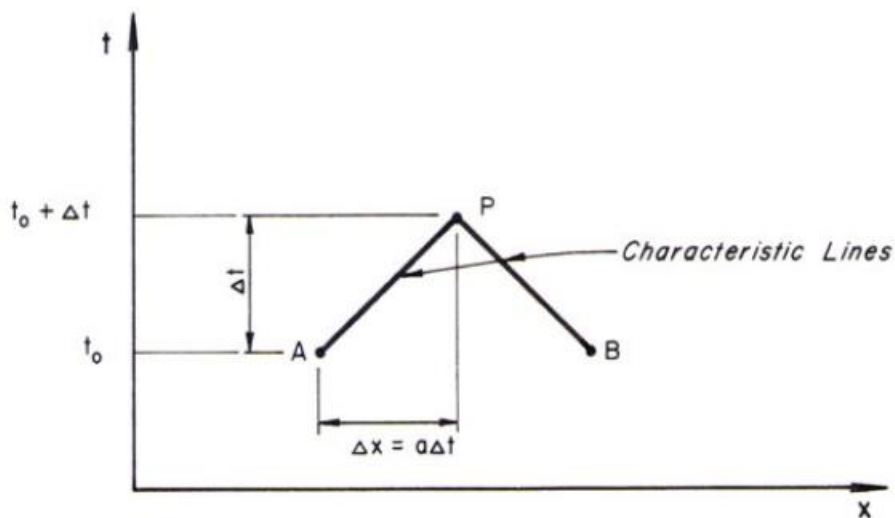


Figure 31 Characteristic lines in x - t plane.

Assuming that the head (H) and discharge (Q) at time $t=t_0$ are known. These values could either be initially specified (i.e., at $t=0$, as initial conditions) or calculated during the previous time step. The objective is to compute the unknown values of (H) and (Q) at time $t=t_0+\Delta t$. Referring to Figure 32, considering that the values of (Q) and (H) are known at points A and B, the aim is to determine their values at point P. This can be achieved by solving Equations 4.1 and 4.2 as follows: By multiplying the left-hand side of Equation 4.1 by dt and integrating, resulting in Equation 4.3:

$$\int_A^P dQ + gA \frac{1}{a} \int_A^P dH + R \int_A^P Q|Q|dt = 0$$

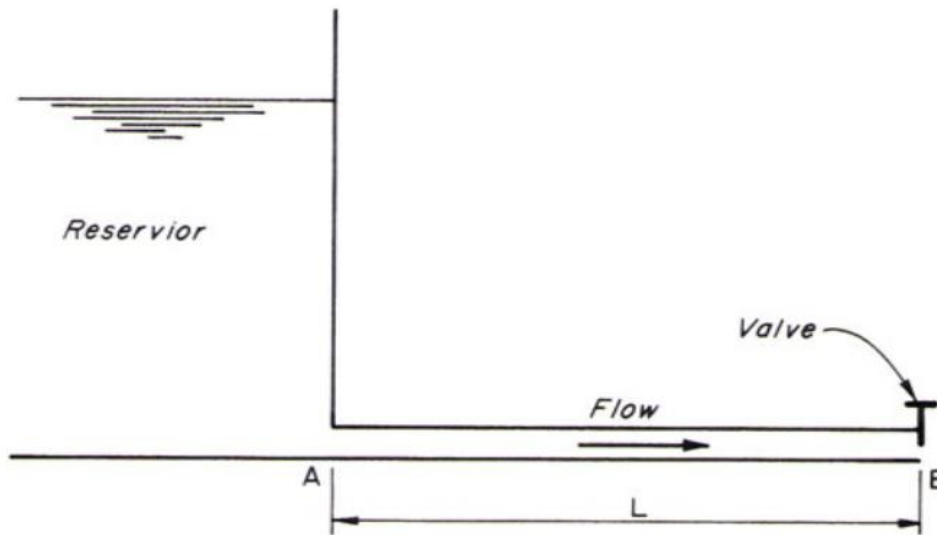


Figure 32 Pipe system

A and P are used to indicate the positions in the $x-t$ plane, and Q_p is the discharge at P, add to that equation 4.1 is only valid on the characteristic line AP, thus the limit extends from A to P.

The first two integral terms of Equation 4.3 are evaluated. Meanwhile, it's not possible to accomplish this for the third term, which stands for the friction losses, as the variation of Q 's explicit to t . Utilizing a first-order approximation, it's possible to evaluate the third term's integral as follows:

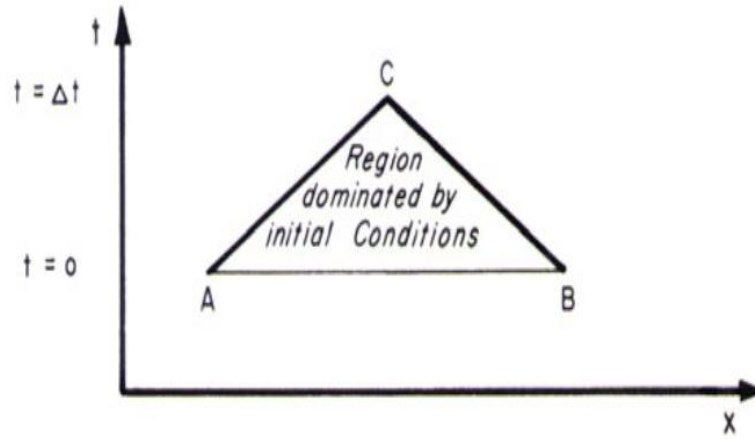


Figure 33 Excitation at the downstream end

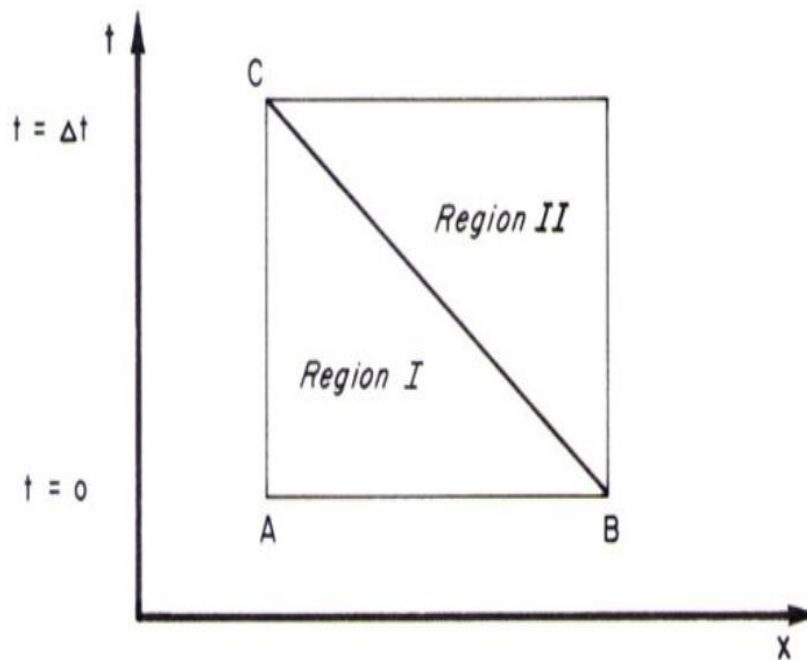


Figure 34 Excitation at the upstream and downstream ends

$$R \int_A^P Q |Q| dt = R Q_A |Q_A| (t_p - t_A) = R Q_A |Q_A| \Delta t$$

Knowing that Q is the same between A and P, Thus equation 4.4 :

$$Q_p - Q_A + gA \frac{(H_p - H_A)}{a} + RQ_A |Q_A| \Delta t = 0$$

It is important to note that Equation 4.4 is precise except for the approximation made for the friction term. This first-order approximation generally provides satisfactory results for most engineering applications. However, this approximation may lead to unstable results if the friction term becomes significantly big. A shorter computational interval Δt can be employed to prevent instability, or a higher-order approximation or an iterative procedure can be used to evaluate the friction term.

For instance, a second-order approximation of the integral of the third term in Equation 4.3 is Equation 4.5:

$$R \int_A^p Q |Q| dt = 0.5 R \Delta t [Q_A |Q_A| + Q_p |Q_p|]$$

Known as the trapezoidal rule. Additionally, there are two other approximations for the friction term Equation 4.6:

$$R \int_A^p Q |Q| dt = R \Delta t [0.5(Q_A + Q_p) + 0.5|(Q_A + Q_p)|]$$

And having Equation 4.7

$$R \int_A^p Q |Q| dt = R \Delta t |Q_A| |Q_p|$$

Since the value of Q_p is unknown, an iterative procedure may be necessary for approximating the equations 4.5 and 4.6. However, the approximation of equation 4.7 results in a linear equation, similar to equation 4.4, which can be solved directly. Following this approach, the expression of $\frac{dQ}{dt} + gA \frac{dH}{-a dt} + RQ|Q|=0$ becomes the following equation 4.8:

$$Q_p - Q_B - gA \frac{(H_p - H_B)}{a} + R \Delta t Q_B |Q_B| = 0$$

By combining all the variables, thus equation 4.5 called the positive characteristic equation is the following:

$$Q_p = C_p - C_a H_p$$

Equation 4.8 called the negative characteristic equation can be written as :

$$Q_p = C_n + C_a H_p$$

Where C_n and C_p are known and remain constant during each time step, although they may change from one-time interval to the next. Meanwhile, C_a is a constant that depends on the properties of the conduit. are the following:

$$C_p = Q_A + gA \frac{H_A}{a} - \Delta t R Q_A |Q_A| \Delta t$$

$$C_n = Q_B - gA \frac{H_B}{a} - \Delta t R Q_B |Q_B| \Delta t$$

Where:

$$C_a = gA \frac{1}{a}$$

However, there are still two unknowns, H_p and Q_p , present in both the positive and negative characteristic equations. Solving these equations will yield the values of H_p and Q_p .

$$Q_p = 0.5(C_p + C_n)$$

The value of H_p can be determined from either $Q_p = C_p - C_a H_p$ or $Q_p = C_n + C_a H_p$. By using $Q_p = C_p - C_a H_p$ and $Q_p = 0.5(C_p + C_n)$, we can calculate H_p and Q_p at all interior points at time $t_0 + \Delta t$ (Figure @). However, at the boundaries, only $Q_p = C_p - C_a H_p$ or $Q_p = C_n + C_a H_p$ is applicable. Therefore special boundary conditions are required to determine the state at the boundaries at time $t_0 + \Delta t$.

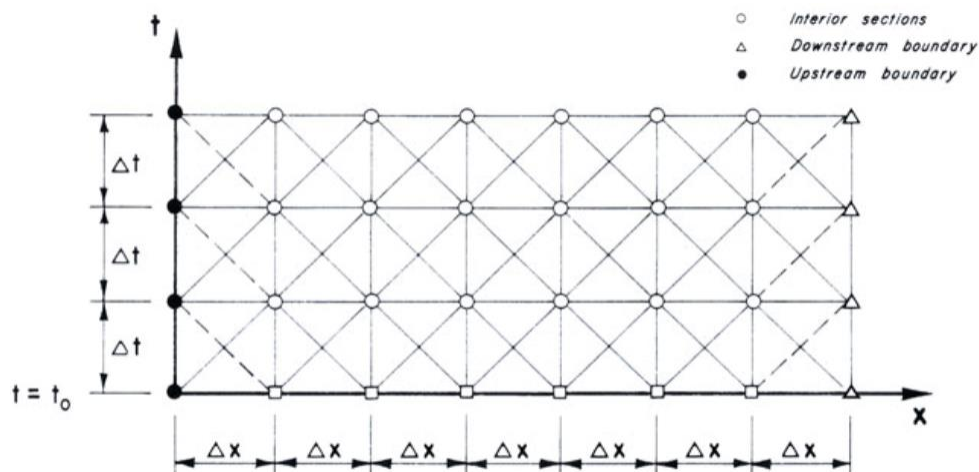


Figure 35 Characteristic Grid

To apply the previous equations, and consider the pipeline shown in Figure 32 (as it is very similar to the present experiment in the laboratory of the LMFA). The pipeline is divided into n reaches Figure 35, each of length Δx . The endpoints of these reaches are referred to as sections, nodes, or grid points. The end sections of each pipe are known as boundaries, while the sections excluding the boundaries are called interior sections, interior nodes, or interior grid points.

First, the steady-state conditions at $t=t_0$ are calculated at all grid points. Then, to determine the conditions at $t = t_0 + \Delta t$, $Q_p = 0.5(C_p + C_n)$ and $Q_p = C_p - C_a H_p$ are applied to the interior nodes, while special boundary conditions are used for the end nodes. As shown in Figure 35, the conditions at the boundaries at $t = t_0 + \Delta t$ must be known to calculate the conditions at $t = t_0 + 2\Delta t$ for the interior nodes adjacent to the boundaries.

With the discharge and head known at all nodes at $t = t_0 + \Delta t$, the values of C_p and H_p at $t = t_0 + 2\Delta t$ are computed following the outlined procedure. This step-by-step process continues until the transient conditions for the required time period are determined [6].

8.3 Application and Results

Utilizing MATLAB to conduct a simulation following the method of characteristics (MOC), with input parameters such as initial conditions like the flow rate and valve initial opening. The simulation takes into consideration friction effects, including pipe roughness and factors related to the water reservoir's output, by transforming the partial differential equations into a set of ordinary differential equations along characteristic curves, it's possible to predict how waves travel through the pipe's system and the water variation in the equilibrium chimney. This approach allows for accurately analyzing and forecasting fluid dynamics behavior and simulating the expected experimental results.

Furthermore, the MOC assists in modifying the system successfully. By testing changes and modifications that might occur on the apparatus such as substituting elements like valves or adjusting their initial settings to observe the impact on system performance. The results of the simulation demonstrated the system's behavior under various conditions, providing valuable insights into optimizing system components and improving overall performance.

The resulting outputs are representations of the variation of pressure head H , flow rate Q , and water level in the chimney H_{st} and valve opening A_v throughout 100 seconds due to the sudden closure of the valve over both the upstream and downstream part of the experiment.

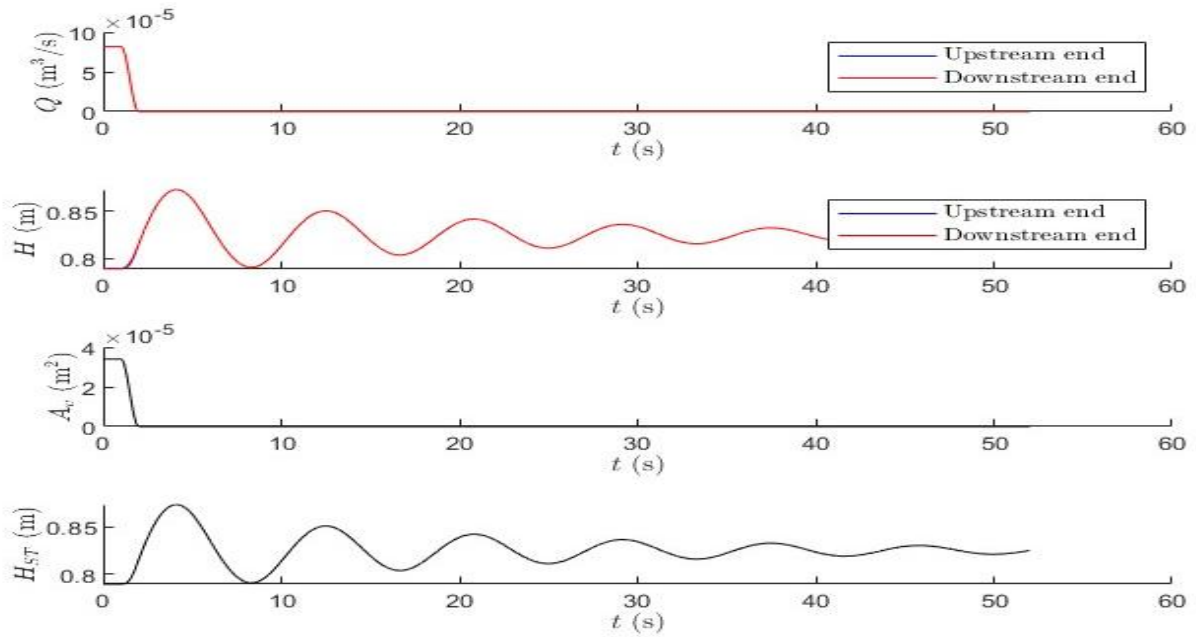


Figure 36 Simulation of the MOC for a flow equal to $8 \times 10^{-5} \text{ m}^3 / \text{s}$

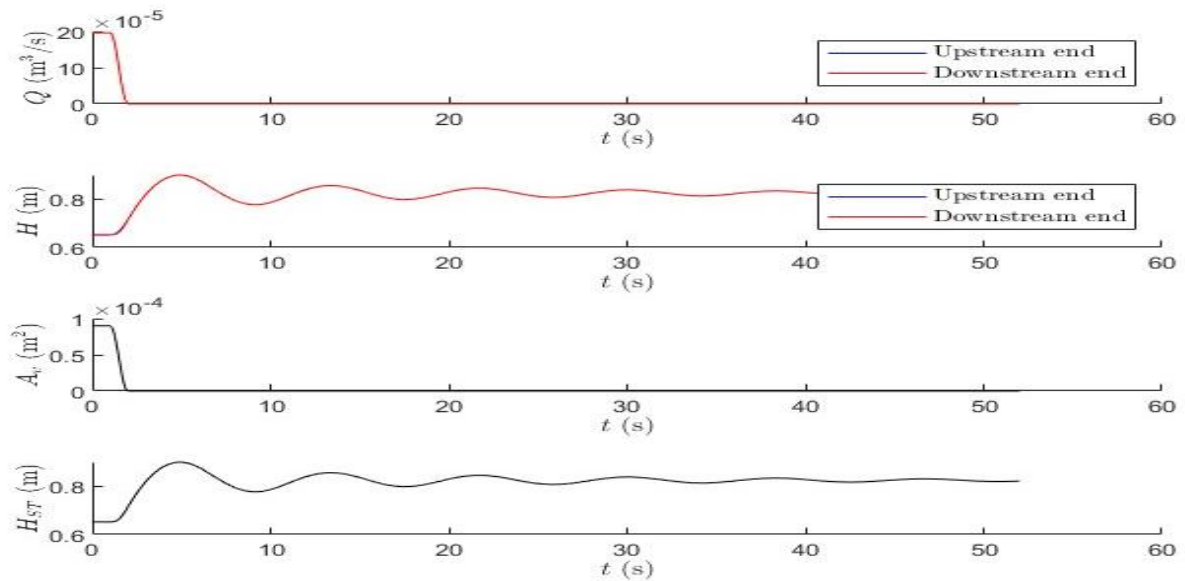


Figure 37 Simulation of the MOC for a flow equal to $1.7 \times 10^{-4} \text{ m}^3 / \text{s}$

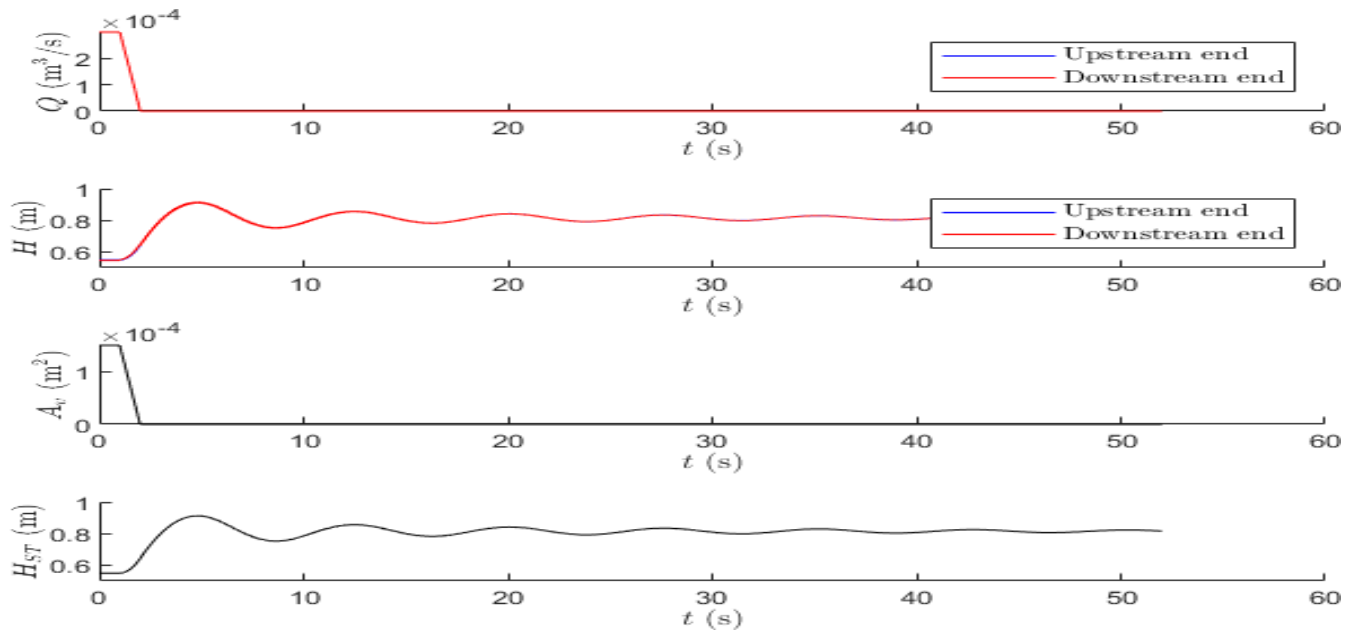


Figure 38 Simulation of the MOC for a flow equal to $2.6 \times 10^{-4} \text{ m}^3 / \text{s}$

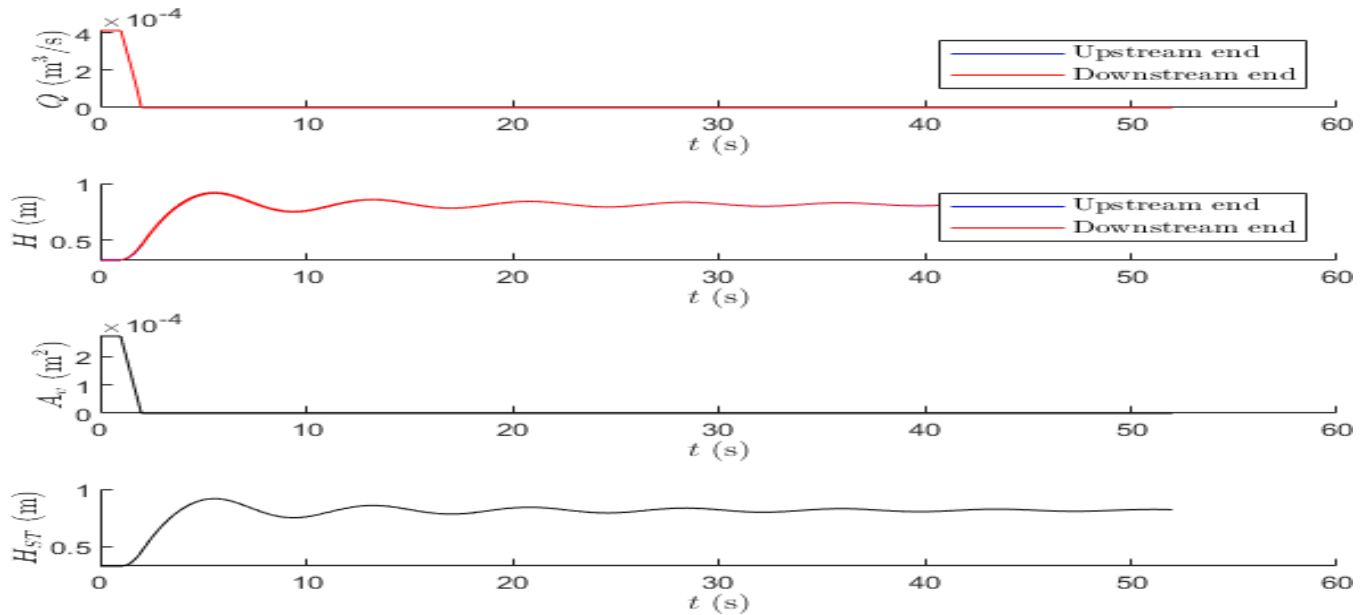


Figure 39 Simulation of the MOC for a flow equal to $4.2 \times 10^{-4} \text{ m}^3 / \text{s}$

The variation we notice in the pressure head is caused by the phenomena of water hammer or coup de belier, and to minimize the effect of the surge the pressure is being dissipated in the chimney that's why we see this increase in water level.

This variation gets greater the bigger the flow rate is, the same scenario we have seen during the conduction of the experiment and the outputs from the numerical analysis even that oscillation period in the method of the characteristic aligns very well with previous analytical and experimental results showcasing that the simulation is correct.

9. Stability check

To ensure that the C7 MkII functions properly and accurately, the experiment must be properly stable. One way to check is by analyzing for differences in water levels on each side of the apparatus the water reservoir and the equilibrium chimney. This method helps detect any leaks, unevenness, or imbalances in the system.

Knowing that there are many ways to check the water level height the fact that it's being measured in this case in a small environment makes it very challenging as a small error or mistake can affect the inaccuracy of the system. That's why it is highly recommended to use high-end technological instruments and avoid low-accuracy methods like tap and equilibrium chimney grading to check the stability.

9.1 Ultrasonic Sensors

One way to measure the water level on both sides with utmost accuracy is by using an ultrasonic sensor suitable for measuring water level in narrow areas, particularly focusing on verifying the water level variation in the experiment. The chosen sensor will play a pivotal role in validating and confirming the accuracy of data derived from the experiment designed to educate students about the phenomenon of water hammer.

To ensure the credibility and reliability of the experimental data, the selection of a precise and accurate ultrasonic sensor is crucial. The sensor will enable real-time monitoring and measurement of water level variations, facilitating the verification of the stability of the experiment and enhancing the educational experience for students learning about water hammer.

Add to that, the chosen ultrasonic sensor must include high accuracy, reliable performance, ease of integration into the laboratory setup, and the ability to measure water level variations with precision. Adaptability for any future modification of the experiment is applied such as the replacement of the old valves with new ones.

9.2 Ultrasonic Sensor Description

The ultrasonic sensor is a device that uses ultrasonic sound waves to measure the distance of a surface or object through air without touching it. It operates by emitting ultrasonic waves and then calculating the time it takes for those waves to bounce back after hitting the surface. By measuring the time taken for the signal to return and knowing the speed of sound in the air, the sensor can determine the distance to the surface.

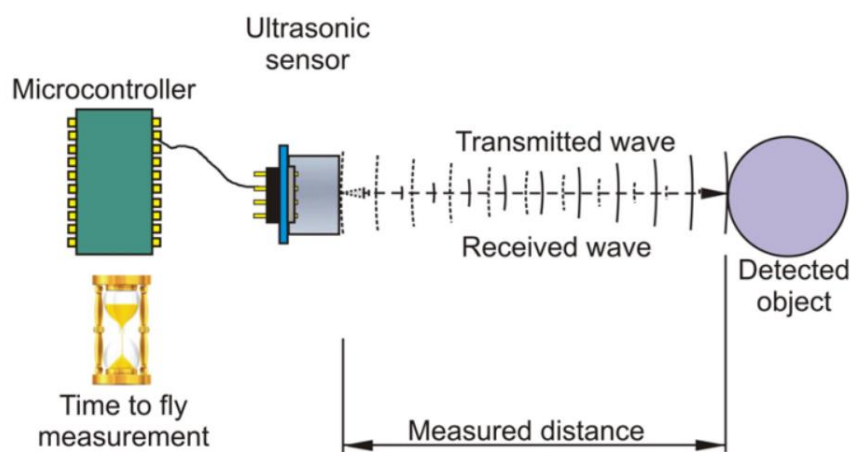


Figure 40 Ultrasonic sensor measurement scheme [9]



The ultrasonic sensor functions as follows:

Ultrasonic Wave Emission: The sensor emits ultrasonic waves, which are high-frequency sound waves, in a certain direction. These waves operate at frequencies higher than human hearing, so humans can't hear them, and travel through the air until they come into contact with a surface or an obstruction.

Waves Reception: The ultrasonic waves are reflected toward the sensor when they come into contact with a surface or an item. Calculating distance requires knowing how long it takes for these waves to return to the sensor after bouncing off an object or surface.

Distance Calculation: The sensor measures the time interval between sending out the ultrasonic wave and receiving its reflection. It precisely measures the time taken for the wave to travel to the object and back. This time measurement is typically done using the speed of sound in the environment (air, water, etc.). Based on the time it takes for the waves to return, the sensor determines the distance to the object by using the known speed of sound in the environment.

Applications for ultrasonic sensors are many and include robotics, industrial automation, car parking systems, liquid level measurement in tanks and reservoirs, object detection, and distance measuring. Their precision, dependability, adaptability for a variety of situations, and non-contact nature make them popular. These sensors are available in several varieties and styles, full of features and functionalities that suit every particular use case and sector.

9.3 Senix Ultrasonic Sensor Selection

9.3.1 Company Introduction

One of the most well-known innovators in ultrasonic sensor technology is Senix Corporation. Senix has established itself as a top manufacturer and supplier of high-quality ultrasonic sensors for various commercial and industrial applications throughout its illustrious thirty-year existence. It is renowned for coming up with innovative solutions, and building robust, trustworthy, and precise sensors that can detect objects, gauge distance, and sense level; it is also committed to providing high-quality products and is always pushing the boundaries of ultrasonic technology. It provides cutting-edge sensor solutions that are specially made to satisfy the increasing demands of various industries throughout the world.



Figure 41 Senix Corporation Logo

9.3.2 Senix Products

Senix offers a wide range of ultrasonic sensor options with different specs, dimensions, and costs based on the required tasks, allowing us to choose sensors that align precisely with our scope of need and requirements.







Ranges					
3 Ft.	14 Ft.	30 Ft.	50 Ft.	50 Ft.	50 Ft.
					
ToughSonic 3	ToughSonic 14	ToughSonic 30	ToughSonic 50 (rear mount)	ToughSonic 50 (clamp mount)	ToughSonic 50 (front & rear mount)
Max. Range 3 ft. (91 cm) Optimum Range 1.75 to 24 in (4.6 - 61cm) Deadband < 1.75 in	Max. Range 14 ft. (4.3 m) Optimum Range 4 in to 10 ft (100mm - 3m) Deadband < 4 in	Max. Range 30 ft. (9.1 m) Optimum Range 10 in to 20 ft (25.4 cm - 6.1 m) Deadband < 10 in	Max. Range 50 ft. (15.2 m) Optimum Range 1 ft to 33 ft (30.5 cm - 10 m) Deadband < 1 ft	Max. Range 50 ft. (15.2 m) Optimum Range 1 ft to 33 ft (30.5 cm - 10 m) Deadband < 1 ft	Max. Range 50 ft. (15.2 m) Optimum Range 1 ft to 33 ft (30.5 cm - 10 m) Deadband < 1 ft
Features					
<ul style="list-style-type: none"> • 316 Stainless Steel • Available in either 30mm or 1" NPT threads (w/o nuts) • R5232 or R5485 • 6 Wire Sensor <ul style="list-style-type: none"> - Power - Serial Interface - 2 Configurable outputs - Teach Button 	<ul style="list-style-type: none"> • 316 Stainless Steel • Available in either 30mm or 1" NPT threads (w/o nuts) • R5232 or R5485 • 6 Wire Sensor <ul style="list-style-type: none"> - Power - Serial Interface - 2 Configurable outputs - Teach Button 	<ul style="list-style-type: none"> • 316 Stainless Steel • 1.5" NPT threads • R5232 or R5485 • 9 Wire Sensor <ul style="list-style-type: none"> - Power - Serial Interface - 5 Configurable outputs - Teach Button 	<ul style="list-style-type: none"> • 316 Stainless Steel • 1.5" NPT threads, rear mount • R5232 or R5485 • 9 Wire Sensor <ul style="list-style-type: none"> - Power - Serial Interface - 5 Configurable outputs - Teach Button 	<ul style="list-style-type: none"> • 316 Stainless Steel • Clamp Mount • R5232 or R5485 • 9 Wire Sensor <ul style="list-style-type: none"> - Power - Serial Interface - 5 Configurable outputs 	<ul style="list-style-type: none"> • PVC • 2.5" NPT threads, front and rear mount • R5232 or R5485 • 9 Wire Sensor <ul style="list-style-type: none"> - Power - Serial Interface - 5 Configurable outputs

Figure 42 Senix products catalog

This diverse catalog allows the making of ideal decisions, selecting sensors that meet the requested technical specifications and align with the lab's budget, ensuring optimal performance while being cost-effective for the projects.



Figure 43 ToughSonic 3

Addressing this specific case of measuring water level variations in a reservoir during pumping operations and controlled discharge, the ToughSonic 3 is an ideal solution. Its 0.086 mm resolution and nominal repeatability of 0.2% of the range at constant temperatures precisely match the needed requirements. With the measured water variation ranging from 10 to 5 centimeters, the ToughSonic 3's optimal range (4.6-61 cm) and deadband (1.75 inch / 4.44 cm) align perfectly with our reservoir's geometry.

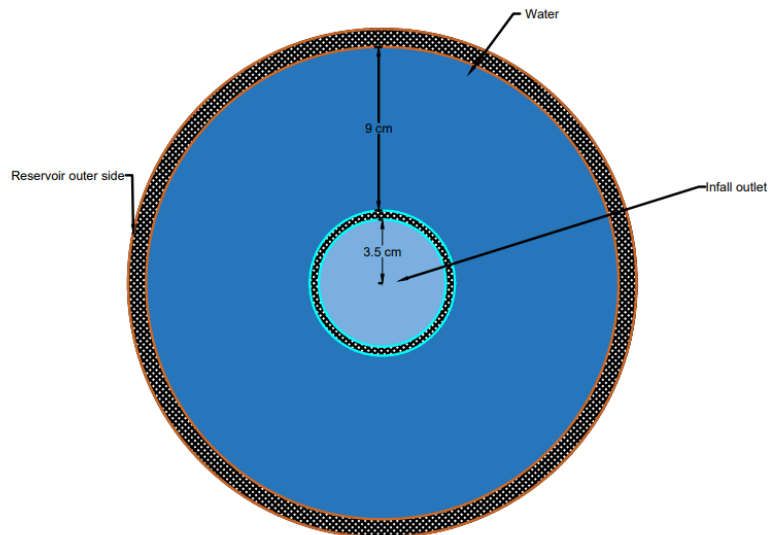


Figure 44 Reservoir Cross-section



Figure 45 Reservoir Measurement

Considering the distance between the reservoir's inner cylinder and the output tube (9 cm), the dead band's compatibility (4.44 cm), and the sensor's conically shaped beam angle (typically 10-15 degrees), ensuring the emitted and received beam remains isolated within the desired measurement area.

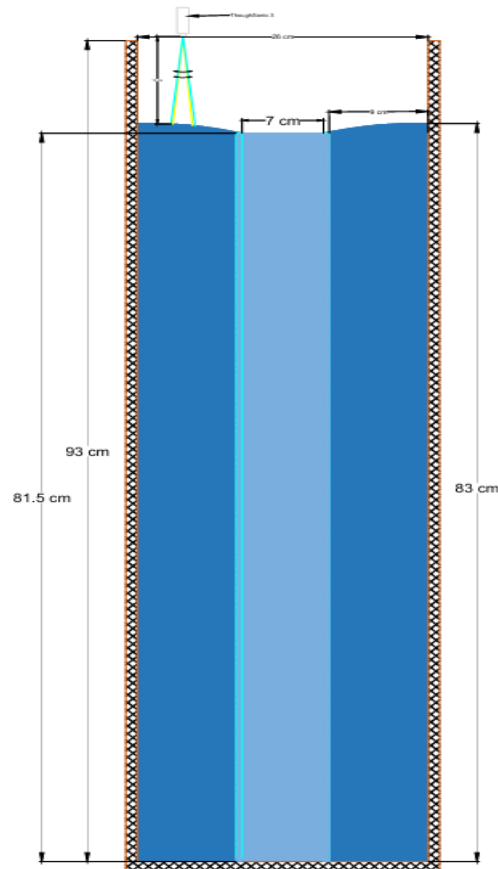


Figure 46 Water reservoir side while using the ThoughtSonic 3

Furthermore, the sensors can detect and mitigate the impact of unintended obstructions or surfaces by adjusting beam width, and sensitivity, and employing processing filters, thus ensuring accurate measurements in complex environments. Additionally, the sensors' immunity to loud sounds and humidity, coupled with a reliable update rate of 20 Hz (50ms), further solidifies their suitability for our intended application.

When conducting the experiment water drops remain on the inner side of the chimney in this case using an inadequate sensor can detect these drops and generate misleading data that ruins the purpose of the experiment

9.3.3 Optimization and Filtering

In case of water agitation in the reservoir caused by the infall (output) or the water pumping (input) filters can be utilized to calibrate the sensor and neglect the jittery readings, filtering includes stability test, averaging type, and delayed reaction types. Simple averaging the last 25-30 measurements smooths the jittery data and the output data from the sensor is configured running rate.

Before average filtering, input rejection filtering is applied, the last ignores many measurements and the total of the collected measurement data is called raw data and the result is the output data. Knowing that the level is varying between 10 and 5 cm any data that does not fit this domain can be filtered and eliminated. This filter is also useful to disregard any unwanted object that interferes between the sensor and the water surface.

Suppose an averaging filter is used for the data received from the input rejection filters. This filter suspends the current distance until stability returns in case an unstable target is caught by the stability filter making it possible also to measure the variation in the chimney of the experiment which has a diameter of 44 mm.

9.4 Pressure Measurement

The water hammer experiment includes a chimney that is used to check the pressure in the pipe when closing and opening the valve to check the surge and show its effect to the students experimenting. Yet when closing the valve, the water level in the surge varies and when the closing is fast it's very hard to observe the water variation and collect data even when taking video records,

thus an easier way to measure the level along the course of the experiment is to use the pressure measurement sensor.

The advantages of utilizing this sensor are multifaceted. By directly measuring pressure, it provides a direct and accurate representation of the water level changes throughout the experiment. This not only eliminates the intricacies associated with visually tracking fast-changing water levels but also offers a more accessible and efficient means to monitor the dynamic phases of the experiment. The sensor's real-time capabilities further contribute to the precision of data capture, ensuring that all variations in pressure are accurately recorded, thereby enhancing the overall reliability and comprehensiveness of the experimental observations.

9.4.1 Pressure Measurement Sensor.

The device is to be set under the water chimney and it will record the pressure in the reservoir and chimney. Knowing the pressure the water level can be determined in both, the reservoir and chimney. The sensor output is set between 4 to 20 mA because, in case of a malfunction or power failure, the sensor won't record any data unlike if it's set for DC 0 to 5 V, a non-linearity between equal to 0.25 % and a measurement range that can reach from between 0 - 0.05 to 0 -1,000 bar ideal to the experimental application.



Figure 47 pressure measurement sensor A-10.

Having similar sensors already installed in the experiment for the fast closure valve, it will be easy to calibrate and use this sensor especially when all required equipment is already present in the lab (computer, cables, and software) also it costs around 75 €, much cheaper than other counterparts and easy installation procedure.

9.5 Alternative Methodologies

Other devices and methods can be considered to measure the water level in the chimney and water tank, but each type comes with a challenge, and not all of them can be overcome easily. Some of these devices were:

Resistance capacitance: It is very hard to achieve accurate measurements in a confined space and implementing the experiment in the installation is no different due to the small diameter of the chimney (44 mm) using resistance-capacitance. Depending on the specific RC circuit design and components used, there may be limitations in the range and resolution of water level measurements. Thus, making this method very complex compared with its other counterparts.

Float Sensors: Float sensors operate based on the principle of buoyancy and are capable of detecting water levels. They can be cost-effective and simple to use. However, their precision and suitability for high-precision measurements, especially in transient phenomena like water hammer, might be limited compared to ultrasonic sensors.

Piezometer: Piezometers measure liquid pressure at a specific point and can indirectly indicate water levels by assessing the pressure exerted by the water column. They offer a direct measurement of the hydraulic head but might necessitate careful calibration and consideration of the container's geometry to accurately infer water levels. In the context of water hammer experiments, piezometers could provide valuable pressure data, but their direct translation to precise water level measurements might require additional calculations or considerations.

The selection of alternative devices for water level measurement in water hammer experiments significantly influences both the cost-effectiveness and overall success of the project. This evaluation necessitates a balanced consideration of various factors. Cost considerations weigh the budget constraints against precision and reliability, highlighting potential economical options like pressure transducers and float sensors.

10. Valves

10.1 Brief Description of Valves

The integration of a digital valve into the laboratory's water hammer experiment aims to enhance precision and efficiency by increasing the interface with the experiment. Currently reliant on traditional valves, the experiment lacks the necessary control over closure dynamics, hindering accurate data collection and reproducibility. The incorporation of a digital valve is expected to address these limitations by providing programmable closure rates, real-time monitoring capabilities, and improved control over experimental conditions. Following a thorough evaluation, the Parker-Lucifer electro-valve is recommended for its wide closure speed range, exceptional accuracy, and compatibility with existing laboratory systems.

This report's secondary objective is to optimize the instrumentation used for measuring water levels in the water hammer experiment's chimney. The current setup lacks the requisite precision, impacting the alignment of data with the experiment's intended outcomes. To overcome these challenges and enhance the accuracy of measurements, the selection of an appropriate device or method is needed. The chosen instrumentation should not only provide precise data but also seamlessly align with the experiment's objectives. Through an evaluation process, the aim is to identify the most suitable device or method that complements the water hammer experiment, ensuring accurate and meaningful data collection.

The key benefits include precise control over the experiment, continuous monitoring of pressure changes, and enhanced reproducibility of experiments. These upgrades align with the laboratory's commitment to scientific advancement and promise to contribute significantly to understanding fluid dynamics all while taking the cost and budget into consideration.

10.2 Valves

A valve is a mechanical device used in systems to regulate the flow of fluids (gases or liquids) through pipes or passages. In several industries, such as manufacturing, energy, and chemical processing, valves are crucial parts. They can be manually, mechanically, or electrically controlled and are used to start, halt, or adjust the fluid flow. Gate valves, ball valves, butterfly valves, and globe valves are among the several types of valves available. These valves are made for certain

uses depending on variables like fluid type, pressure, and temperature. A valve's main job is to regulate the flow's direction and rate to keep a fluid system operating safely and effectively.

Digital valves, on the other hand, represent a technological advancement in fluid control systems. Unlike their traditional counterparts, digital valves utilize electronic or computerized control mechanisms for precise and programmable operation. They offer the capability to modulate flow rates, enable remote control, and allow for real-time monitoring of various parameters such as pressure and temperature. Digital valves contribute to enhanced automation, providing greater accuracy and repeatability in regulating fluid flow.

The key difference lies in the control mechanism: traditional valves rely on manual or mechanical operation, while digital valves leverage electronic control systems. This distinction grants digital valves the ability to offer finer adjustments, programmable settings, and integration with modern automation technologies. As a result, digital valves are particularly beneficial in applications where precise control, automation, and real-time monitoring are critical factors for operational efficiency and experimental accuracy.

Here is a general overview of how an electro valve (solenoid valve) works:

Solenoid Mechanism: The electro valve is made from a moveable ferrous core, also known as a piston, that is encircled by a wire coil. A magnetic field is produced by the coil when an electric current is introduced to it. The ferrous core moves because of the activated coil's magnetic field drawing it in and due to this axial movement closes the valve.

1. **Valve Operation:** The movement of the core affects the position of the valve's internal components. In a basic solenoid valve, there is a seal or diaphragm that is either lifted or lowered by the movement of the core. This action opens or closes the passage for the fluid, controlling the flow through the valve. The opening and closing of the valve are rapid and precise, making electro-valves suitable for applications requiring quick response times and accurate flow control.
2. **Power Shutdown:** When the electric current is turned off, the magnetic field dissipates, and the spring or other mechanical components may return the core to its original position. This action results in the opening of the valve returning [3].

10.3 Valve selection

10.3.1 Company Introduction

Parker Valves stands at the forefront of valve technology, distinguishing itself as a vanguard in the industry. With a legacy marked by ingenuity and excellence, Parker Valves has firmly established its standing as a preeminent manufacturer and supplier of high-grade valves. The company is lauded for its unwavering commitment to pioneering solutions, consistently engineering valves that embody not just robustness and dependability, but also precision-crafted sophistication in regulating fluid dynamics across diverse industrial terrains. Parker Valves remains dedicated to delivering products of unparalleled quality, continually pushing the boundaries of valve technology to meet the dynamic and evolving demands of industries on a global scale. Through avant-garde valve solutions, Parker Valves adeptly tackles the multifaceted challenges inherent in various sectors, cementing its reputation as a trusted and forward-thinking force shaping the ongoing narrative of valve innovation.



Figure 48 Parker Lucifer Corporation Logo

10.3.2 Electro-valve 221G/15

Following a meticulous evaluation of numerous products and thoughtful consultations with various producers and providers, the best choice for measuring water levels in the chimney during the water hammer experiment emerges in the form of the 221G electro-valve. This exceptional device stands as a testament to versatility and reliability, seamlessly aligning with the experiment's lofty objectives.

The 221G electro-valve distinguishes itself with a plethora of features that render it an unparalleled candidate for this application. Its ingeniously designed mechanism not only simplifies the installation process, allowing for the seamless substitution of the old valve but also facilitates effortless integration into diverse experimental setups. This adaptability becomes the cornerstone, ensuring that the electro-valve can adeptly navigate the dynamic conditions within the chimney, guaranteeing the acquisition of accurate and responsive measurements.

What sets the 221G electro-valve apart is not only its adaptability but also its remarkable operational efficiency. With the capability to close and open within a mere 30 ms and 35 ms, respectively, this electro-valve emerges as the quintessential instrument to meticulously observe the water hammer experiment and meticulously collect data. The valve's dimensions, boasting an opening diameter of $\frac{1}{2}$ " , coupled with its user-friendly design, further solidify its status as an ideal instrument for our experiment.



Figure 49 221 G /15 electro-valve

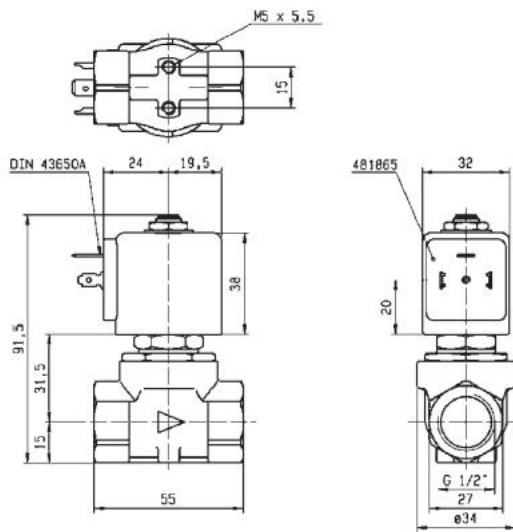


Figure 50 221 G 15 Sections [4]

Another crucial consideration for selecting this valve lies in its installation process, which mirrors that of the existing valve already in place. This seamless integration eliminates the need for additional modifications or adjustments, streamlining the implementation and ensuring continuity in the experimental setup so that the total cost of the valve does not surpass 100 € (while the motor-driven valve costs around 450€) much lower than other valves in term of cost and time efficiency.

10.4 Simulation in case of a full-flow

The 221G electro-valve has an inner diameter of 0.5 inch (1.27 cm thus the area of a full opening AD is 1.26 cm^2) and a closing time of 30 ms. Knowing that the closing blade of the valve sections closes in the form of a guillotine thus we won't have a linear decrease in the valve's open cross-section area (A_v) when closing the valve. Thus, using MATLAB, we were able to get the following scheme:

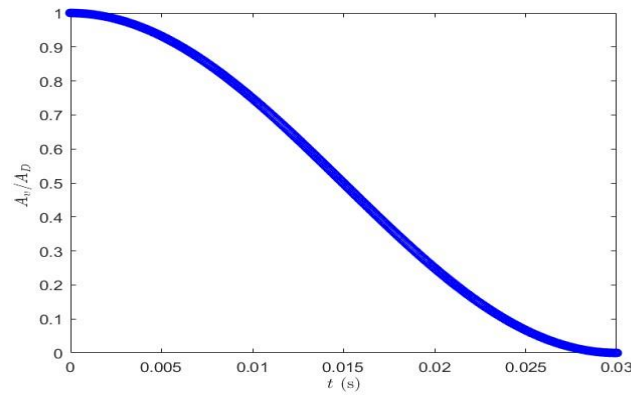


Figure 51 Valve opening area variation in function of time of closure.

Knowing that the analytical formula applied for the area of the closing of the valve is the following:

$$A_v = \frac{A_i}{2} \cos t + \frac{A_i}{2}$$

The parameters are the following:

A_v : valve current open at time t

A_i : valve initial opening

And applying the method of the characteristics for an initial full opening of the valve and full closure within 30 ms we can get preliminary results of how the experiment will look like and the observations we will witness, especially what's related to the water level variation in the chimney.

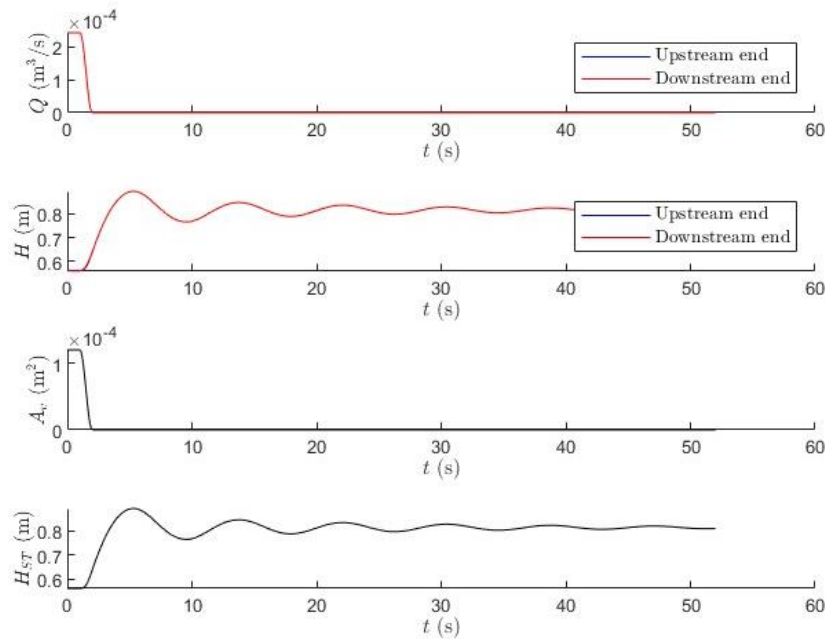


Figure 52 Simulation in case of a total valve opening

And we can deduce the information regarding the flow such as a maximum flow of 0.24 liters per second, the oscillation period of about 9 seconds, and the water level in the chimney at each moment of the experiment with an initial water level of 562 mm. And in case we are not satisfied with these results we can always change the valve by choosing from the series a valve with a different opening area like the 221 G /25.

Parker offers a wide range of valves that even need the same valve but with a different diameter or closing/opening speed it's easy to find our product without the need to search for another supplier or enterprise. The catalog below highlights some of their products that are particularly pertinent to our objectives.

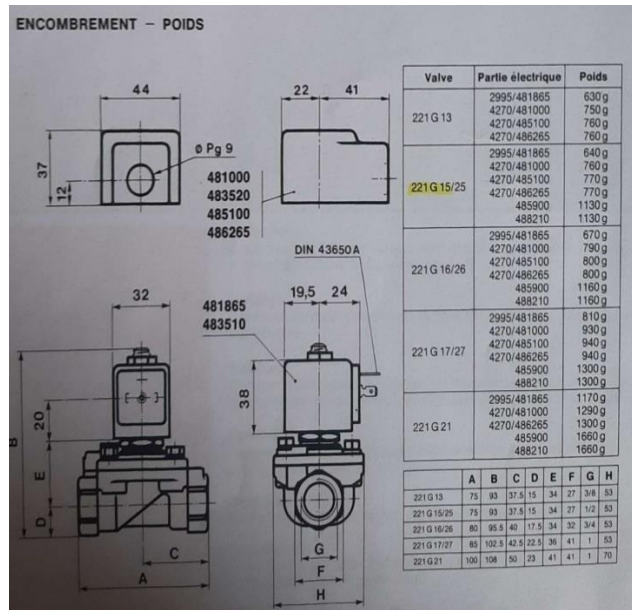


Figure 53 Valves catalog.

Type	Pos.	Ouverture (s)	Fermeture (s)
221 G 13		0.030	0.350
221 G 15/25		0.030	0.350
221 G 16/26		0.040	0.360
221 G 16 10	1	0.035	0.200
	2	0.035	0.410
	3	0.030	0.900
	4	0.030	1.750
221 G 17/27		0.035	0.370
221 G 17 10	1	0.050	0.220
	2	0.050	0.350
	3	0.045	0.800
	4	0.040	1.700
221 G 21		0.100	0.900
221 G 21 10	1	0.170	0.550
	2	0.130	0.950
	3	0.090	2.000
	4	0.070	4.000

Figure 54 All Valve opening and closing times.

10.5 Alternative Valves

Several alternative valves and methodologies exist that can effectively fulfill the necessary tasks. Some of these alternatives present viable options to consider alongside ultrasonic sensors for accomplishing the desired tasks.

- **Motor-driven valves:** This valve's opening and closing are done by gears connected to a motor. The main problem with this valve is the time it takes. For example, to close the valve it takes a few seconds. At this point, the experiment would be useless, it wouldn't have the water phenomenon and would cost a lot compared to its other counterparts.



Figure 55 Motor-driven valve [10]

- **Angle seat globe valve:** The globe valve is mainly set to modulate and control water flow but also prevent water hammer cases, so it does not fit with the scope of the experiment since it removes the water hammer phenomena and defeats the experiment's purpose.



11. Conclusion and Future Work

This thesis research aims to deepen our understanding of fluid dynamics by focusing on the variation of water levels in a chimney and reservoir under different flow conditions. Analytical analyses and calculations were conducted for this purpose to check the execution of the experiment if the results are as expected when experimenting in real-time. Using the experimental setup ensured precision in both construction and analysis. We conducted experiments with varying flow rates and utilized cameras to capture and measure water level variations. This approach generated a detailed dataset that highlights the dynamic relationship between flow rates and oscillation amplitudes, ensuring the accuracy and reliability of our measurements.

By applying the Method of Characteristics (MOC), we were able to transform complex partial differential equations into more manageable ordinary differential equations along characteristic curves. This enabled us to accurately predict the system's behavior, providing valuable insights into wave-like phenomena in fluid dynamics and comparing the results with the analytical analyses.

We suggested and studied many methods to measure the water level on both sides to check the stability of the experiment. During the search for the best tool to measure the water level, several methodologies and devices from different brands in the market were studied and evaluated to check if they were compatible with the aim of this project. If a balance is made between cost-effectiveness, accuracy, educational impact, and long-term viability, the choices mentioned in this thesis emerge as the optimal choices. Their precision, range compatibility, and align perfectly with our project objectives. These upgrades ensure accurate data collection and enhance the educational experience, making it the ideal device to support our study of water hammer phenomena in fluid dynamics experiments.

To further enhance our control over the experimental apparatus, we propose the implementation of a new valve installation. This innovative valve is expected to provide better regulation of flow rates, allowing for more precise adjustments and improved overall interface with the system. Testing and comparing the new valve with the existing one will help us assess its impact on the accuracy and stability of the experiments.

Future studies could investigate the impact of different valve designs and materials on system performance. This includes experimenting with smart valves that can be remotely controlled and



adjusted in real-time to dynamically optimize flow conditions. Additionally, employing computational fluid dynamics (CFD) simulations in conjunction with the Method of Characteristics (MOC) to develop hybrid models is a promising direction. Such models could leverage the strengths of both approaches, leading to more precise and efficient simulation tools for predicting complex fluid behaviors.

Experimental validation of these advanced models in large-scale or industrial applications would provide valuable insights and practical benefits, ultimately contributing to advancements in fluid dynamics research and engineering solutions. By integrating precise measurement techniques, the application of MOC, and innovative valve designs, this research significantly contributes to the field of fluid dynamics.

The findings will not only validate the effectiveness of the MOC in predicting fluid behavior but also improve experimental methodologies. Ultimately, this work aims to advance both the theoretical understanding and practical applications of fluid dynamics, paving the way for future innovations and developments in the field.

12. References

- [1] F. Wood, History Of Water-Hammer, Ontario: QUEEN'S UNIVERSITY AT KINGSTON, 1970.
- [2] J. Martínez, Real-time Monitoring of Water Levels using IoT Technologies, 2018.
- [3] R. W. Zappe, "Valve Selection Handbook: Engineering Fundamentals for Selecting the Right Valve Design for Every Industrial Flow Application," Elsevier, 2004.
- [4] P. H. Corporation, General Catalogue Solenoid Valves for Fluid Control, 2022.
- [5] M. S. Ghidaoui, A Review of Water Hammer Theory and Practice, 2005.
- [6] M. Hanif Chaudhry, Applied Hydraulic Transients Third Edition, Columbia, SC, USA: Springer, September 24, 2013.
- [7] Xaintrie-Passions, [Online]. Available: <https://www.xaintrie-passions.com/chemin%C3%A9-%C3%A9quilibre/>. [Accessed 2024].
- [8] Armfield, C7 MKII Pipe surge and Water hammer Apparatus - Armfield., 2023, February 6.
- [9] I. V. T. K. L. M. P. F. T. L. M. L. Michal Kelemen, "Science and Education Publishing," 2015. [Online]. Available: <https://pubs.sciepub.com/automation/3/3/6/figure/1>.
- [10] "Danfoss Motorized control valves and actuators," [Online]. Available: <https://www.danfoss.com/en/products/dhs/valves/motorized-control-valves-and-actuators/#tab-overview>. [Accessed 2024].